Peridotite Weathering and Ni Redistribution in New Caledonian Laterite Profiles: Influence of Climate, Hydrology, and Structure

Michel Cathelineau, Yoram Teitler, Jean-Louis Grimaud, Sylvain Favier, Fabrice Golfier, Erick Ramanaidou, Sylvain Grangeon, Yohann Kerreveur, Julie Jeanpert, Samuel Étienne, et al.

minerals

MDPI

Review

Peridotite Weathering and Ni Redistribution in New Caledonian Laterite Profiles: Influence of Climate, Hydrology, and Structure

Michel Cathelineau [1,*], Yoram Teitler [1,2], Jean-Louis Grimaud [3], Sylvain Favier [1], Fabrice Golfier [1], Erick Ramanaidou [2], Sylvain Grangeon [4], Yohann Kerreveur [4], Julie Jeanpert [5], Samuel Étienne [5], Manuel Muñoz [6] and Marc Ulrich [7]

1 Université de Lorraine, CNRS, GeoRessources, F-54000 Nancy, France; yoram.teitler@univ-lorraine.fr (Y.T.); favier.syl@wanadoo.fr (S.F.); fabrice.golfier@univ-lorraine.fr (F.G.)
2 CSIRO Mineral Resources, ARRC, 26 Dick Perry Avenue, Kensington, WA 6151, Australia; erick.ramanaidou@csiro.au
3 PSL University/MINES Paris/Centre de Géosciences, 35 rue St Honoré, F-77305 Fontainebleau, France; jean-louis.grimaud@minesparis.psl.eu
4 BRGM, 45100 Orléans La Source, France; s.grangeon@brgm.fr (S.G.); yohann.kerreveur3@etu.univ-lorraine.fr (Y.K.)
5 SGNC DIMENC, Nouvelle Calédonie, 1 ter rue Unger Vallée du Tir, 98800 Nouméa, France; julie.jeanpert@eaurmc.fr (J.J.); samuel.etienne@gouv.nc (S.É.)
6 Géosciences Montpellier, Université de Montpellier, CNRS, Campus Triolet, Place Eugène Bataillon, F-34095 Montpellier, France; manuel.munoz@umontpellier.fr
7 Université de Strasbourg, CNRS, Institut Terre et Environnement de Strasbourg, UMR 7063, 5 rue Descartes, F-67084 Strasbourg, France; mulrich@unistra.fr
* Correspondence: michel.cathelineau@univ-lorraine.fr

Abstract: The peridotite massifs of New Caledonia are characterised by complex hydrodynamics influenced by intense inherited fracturing, uplift, and erosion. Following the formation of the erosion surfaces and alteration processes, these processes drive chemical redistribution during weathering; particularly lateritisation and saprolitisation. Magnesium, silica, and trace elements such as nickel and cobalt—released as the dissolution front advances—are redistributed through the system. New observations and interpretations reveal how lateritic paleo-land surfaces evolved, and their temporal relationship with alteration processes since the Oligocene. Considering the geometry of discontinuity networks ranging from micro-fractures to faults, the transfers occur in dual-permeability environments. Olivine dissolution rates are heterogeneously due to differential solution renewal caused by erosion and valley deepening. Differential mass transfer occurs between mobile regions of highly transmissive faults, while immobile areas correspond to the rock matrix and the secondary fracture network. The progression of alteration fronts controls the formation of boulders and the distribution of nickel across multiple scales. In the saprolite, nickel reprecipitates mostly in talc-like phases, as well as minor nontronite and goethite with partial diffusion in inherited serpentine. The current nickel distribution results from a complex interplay of climatic, hydrological and structural factors integrated into a model across different scales and times.

Keywords: laterite; peridotite; erosion surface; saprolite; nickel; cobalt; scandium

Citation: Cathelineau, M.; Teitler, Y.; Grimaud, J.-L.; Favier, S.; Golfier, F.; Ramanaidou, E.; Grangeon, S.; Kerreveur, Y.; Jeanpert, J.; Étienne, S.; et al. Peridotite Weathering and Ni Redistribution in New Caledonian Laterite Profiles: Influence of Climate, Hydrology, and Structure. *Minerals* **2024**, *14*, 1082. https://doi.org/10.3390/min14111082

Academic Editor: Diego De Souza Sardinha

Received: 27 August 2024
Revised: 10 October 2024
Accepted: 21 October 2024
Published: 27 October 2024

1. Introduction

In a hot climate, with an average temperature exceeding 25 °C and high humidity (rainfall of several metres per year), supergene weathering produces a residual soil known as laterite [1–6]. Most laterites were formed during the Cenozoic, with some dating back to the end of the Mesozoic [7–11]. The geometry of laterite fronts developed on peridotites depends on several factors: climate (temperature, rainfall); topography, which influences the water table and hydrological flows; fracturing, which controls underground drainage; and geodynamics, particularly exhumation rates, which affect relief and erosion rates [2,12–14].

Lateritic alteration of peridotites produces specific profiles [15–17]. The divalent iron in the fayalite component of olivine immediately oxidises to trivalent iron, which is insoluble and precipitates as iron oxide and oxyhydroxide. Goethite is the main constituent of the yellow to red horizons comprising the upper part of the laterite profile, usually capped by the lateritic residuum dominated by goethite and hematite. Most major elements (Si, Mg) constituting the bedrock are solubilised following the dissolution of magnesian olivine (forsterite component). These elements may reprecipitate further down as silicates (sepiolite, talc-like minerals, nontronite) or they may be incorporated in previous minerals such as serpentine. In the upper part of the profile (yellow and red laterite), the dissolution of the primary silicates (olivine, pyroxene, serpentine) is gradual. The short residence time of meteoric waters prevents the system from reaching the solubility products of other silicates, leading to the export of Si, Mg, and Ni.

The saprolite is a complex mineral assemblage of oxides, oxyhydroxides, and phyllosilicates in the lower part of the profile. The silicates are, however, very tiny particles—generally no larger than a few hundred nanometres at maximum—which are difficult to identify by methods other than TEM [18–20]. On the other hand, X-Ray absorption spectroscopy is particularly adapted to characterise the behavior of metals in such finely divided material (i.e., oxidation state of iron, and/or the identification of the mineral phases that host metals). Bulk EXAFS analysis revealed that nickel can be present in both oxides and phyllosilicates [21], while in-situ XANES and pre-edge analysis performed on a boulder from saprolite horizon revealed Ni-enrichment of polygonal serpentine [22].

Nickel is present in low concentrations (a few thousand ppm) in the silicates of ultramafic rocks, such as mantle peridotites, primarily in olivine, with lower concentrations in pyroxenes. Serpentines, which form from silicate conversion during subduction or the obduction of peridotites, generally retain the same trace element content. In the upper part of the laterite profile, goethite is the prominent expression of iron, which is insoluble under oxidising conditions. It retains nickel concentrations up to approximately 1.5% but recrystallises in the upper levels of the profiles, resulting in a partial nickel loss from its lattice. Such a process produces a zonation of nickel content associated with goethite ageing [23,24]. Vertical and lateral displacements of nickel in the yellow laterite indicate that nickel distribution is not static, but evolves with time. The competition between vertical and lateral movements is influenced by topography, as water moves according to the relief slope [25].

In the lower part of the alteration profile, silica, magnesium, and nickel are partly reprecipitated as magnesian and nickel-bearing silicates, forming a metric to multi-metric horizon known as “saprolite”, beneath which lies unaltered bedrock. Many significant nickel deposits are associated with the precipitation of magnesian and nickel-bearing silicates, such as those in New Caledonia, Indonesia, and Cuba. In New Caledonia, talc-like, serpentine, and locally nontronite are the predominant Ni-phyllosilicates [19,26,27]. Contrarily, sepiolite and serpentine are dominant in the Dominican Republic and Cuba [20].

In New Caledonia, the historical Ni ore genesis model assumes a single per descensum process, where most of the significant elements constituting the bedrock (i.e., Mg, Ni, and Si) are solubilised through the dissolution of primary magnesian olivine (forsterite) during the development of lateritic soils [28]. This model has been refined by considering the geomorphological context and evolution resulting from the competition between uplift and erosion following the work of [29,30]. Additionally, the classification of mineralisation types by their geomorphological situation (plateau, slope, basin: [31–34] and the role of faults in the redistribution of nickel [35] have further supplemented the model.

However, such a scheme ideally predicts nickel deposits with a simple, zoned structure, characterised by continuous subhorizontal layers parallel to the paleosurfaces from the surface to the depth. In reality, the situation is far more complex due to several factors. The processes involved are multiphase and extend at least 25 Ma [33,36]. Since the obduction of the peridotites, significant changes in relief and climate, including variations in temperature and rainfall intensity, have occurred. These changes, coupled with heterogeneities in the

distribution of fracturing, partly inherited from the obduction stages, need to be considered to understand better the mechanisms of Ni-Co-Sc enrichment over time. Even now, fracture permeability significantly influences meteoric water movements in the peridotites [37,38].

This paper considers the successive scientific advances made over the past decade, which are relatively scattered and often very focused on a single aspect of these complex systems. Figure 1 summarises the main factors to be considered when modelling the formation of nickel enrichments: (i) inherited networks of discontinuities; (ii) the competition between uplift and erosion, which controls valley incisions and relief; (iii) the role of relief on the nature of flows and the geometry of the nappe; (iv) fluid–rock interactions, which, depending on the nature of the newly formed products and the presence of olivine relics, drive the distribution of the pH front, thereby influencing some of the neoformations and nickel enrichment in the form of newly formed silicates. Another factor to consider is the scales of observation and the scaling laws, i.e., the transposability of observations at a given scale to higher scales.

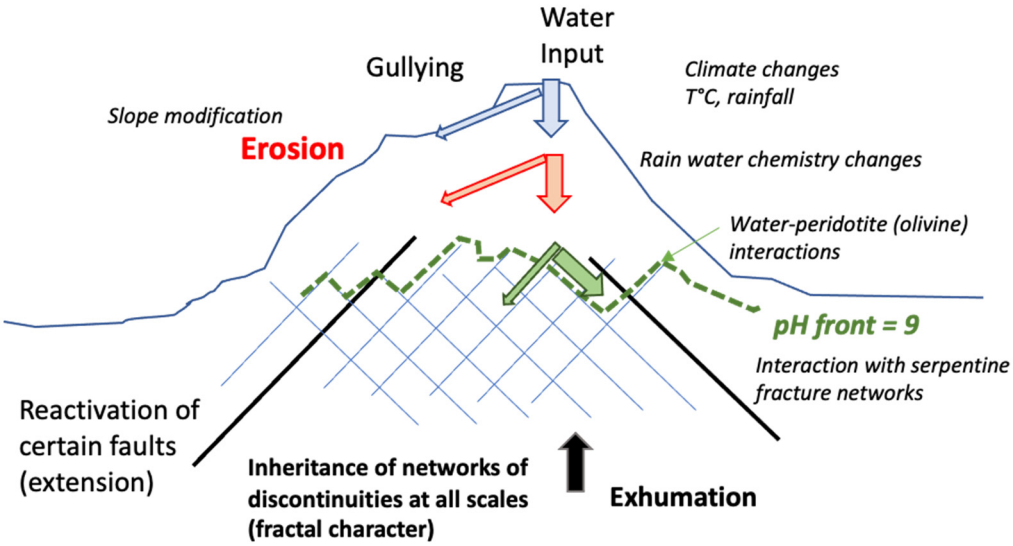

Figure 1. Main parameters controlling the weathering front development and deepening in the context of supergene alteration of peridotites.

In the last decade, several attempts at thermodynamic modelling of water–rock interactions have been proposed [39,40]. However, the complexity of the permeability distribution was not considered until the works of [13,41]. New observations in New Caledonia at a series of representative sites, coupled with advanced modelling, have enabled a comprehensive review of recent results and the proposal of an integrated overall scheme for laterite genesis and related metal enrichment.

2. Materials and Methods

2.1. New Caledonia Geology

New Caledonia, located around 2000 km east of Australia in the South Pacific, constitutes the northernmost part of the Norfolk Ridge. The Norfolk Ridge blocked the Eocene subduction of a marginal basin that had opened further east during the Campanian-Paleocene (90–55 Ma). It was covered by the peridotite nappe, obducted at around 34 Ma [42,43]. The peridotite nappe consists of harzburgites and dunites formed in a supra-subduction zone. Only the massifs in the north of the island are composed of lherzolites [44,45]. The nappe is strongly serpentinised with decreasing intensity from the ductilely deformed sole to the summit, with the development of lizardite, minor chrysotile, then polygonal serpentine in the sole, and numerous lizardite veins and faults in the upper part. The shearing at the sole occurred during obduction, while later serpentine-filled fractures are linked to an oriented extension phase [46]. Ulrich et al. [47] proposed the following chronology of serpentine minerals: after primary syn- subduction lizardite several veins of serpentine minerals related to obduction

are formed, following the order: lizardite 1 → lizardite 2 → antigorite → chrysotile → polygonal serpentine.

Close to the upper parts of the nappe, fractures are predominantly filled by lizardite, which was converted into polygonal serpentine. These two serpentine polymorphs play an essential role in re-opening fractures and infilling new assemblages, which formed subsequently during syntectonic low-temperature hydrothermal stages [19]. Numerous fractures and serpentinised faults linked to the syn- to slightly post-obduction stages were reactivated during compression and extension phases. These fracture networks are essential for the drainage of meteoric fluids responsible for nickel mineralisation, the current degradation of ancient alteration profiles and the formation of the pseudo-karstic system that is still active [14,37,48].

Following the work of Trescases [28], a sequence of stepped lateritic relict paleo-landsurfaces was defined in New Caledonia [49]. The most identifiable ones are ranked from the oldest to the youngest (S1 to S5). Each Sn member of the sequence corresponds to a mosaic of low slope topographic surfaces, hardened by a ferricrete, and that can be found in a given elevation range in the landscape. The ferricrete corresponds to an upper horizon in a lateritic weathering profile. As river incision progresses, the base level for weathering is lowered, and a new lateritic weathering profile is set up. Each Sn surface is, therefore, associated with a different weathering profile. The oldest members of the sequence (i.e., surfaces and associated weathering profiles) are the most elevated. Above 400–600 m in the massif, the nappe is overlain by a highly dissected and partially reworked lateritic profile [31]. It is composed of two residual lateritic surfaces (called S1 and S2) by [30,49], such as in the Tiébaghi plateau further north. Surfaces S3 to S5 are found at lower landscape elevations, i.e., below 400 m.

2.2. Methodology

The morphogenesis associated with deposit emplacement must be considered to understand the multiphase formation of laterite profiles [50,51] and their nickel enrichment. Reconstructing the landscape evolution history consistently with erosion-alteration phenomena and tectonic uplift phases (exhumation-extension) is essential for introducing accurate ranges of relief variation, water table fluctuations, and hydraulic gradients into the models. Before the field mission, a preliminary analysis was conducted based on existing data (relief map and lateritic mapping in the literature). Following the fieldwork, a more exhaustive study of all sites of interest was carried out. Identifying the different lateritic paleo-land surfaces allowed us to specify the impact of surface abandonment/reactivation and determine the role of the incision dynamics on the geomorphological evolution of the study sites. In general, our maps fit well with the ones from [30], as others (e.g., ref. [34] focus less on the relative chronology between lateritic paleo-landsurfaces. In the Southern massif, the mapping was refined compared to previous studies due to the opportunity to make observations directly in mining areas.

The relationships between the nature of macroscopic structures and the heterogeneity of mineral assemblages and grades are characterised at several scales of observation. At the quarry scale, the combination of structural surveys and structural data provided by mining operators facilitates understanding the distribution and spacing characteristics of the prominent fracturing families.

Combining observations using optical SEM and TEM data makes refining the evolutionary model of the mineralogical phases supporting nickel mineralisation easier. The objective of the Transmission Electron Microscopy analyses was to unambiguously determine the nature and evolution of the phyllosilicate carriers of saprolitic mineralisation. Ni carriers in saprolite and laterites were studied near and far from Ni-silicate mineralised structures.

Finally, conceptual and numerical modelling was developed using combined PHREEQC and COMSOL codes [52,53]. The present paper briefly summarises some essential results from the modelling [54].

2.3. Study Sites

The study sites were selected in consultation with the CNRT's mining partners. Based on the good representativeness of the types of deposits in New Caledonia, this choice was made as part of the Transnum project. The sites selected are represented in the map from Figure 2: Pit Cagou (Koniambo, KNS), Nakéty Plateau (SMT), Goro (Prony resources) and Henriette (SMT). Comparisons were made with other previously studied sites, particularly Cap Bocage, Thio and Tiébaghi.

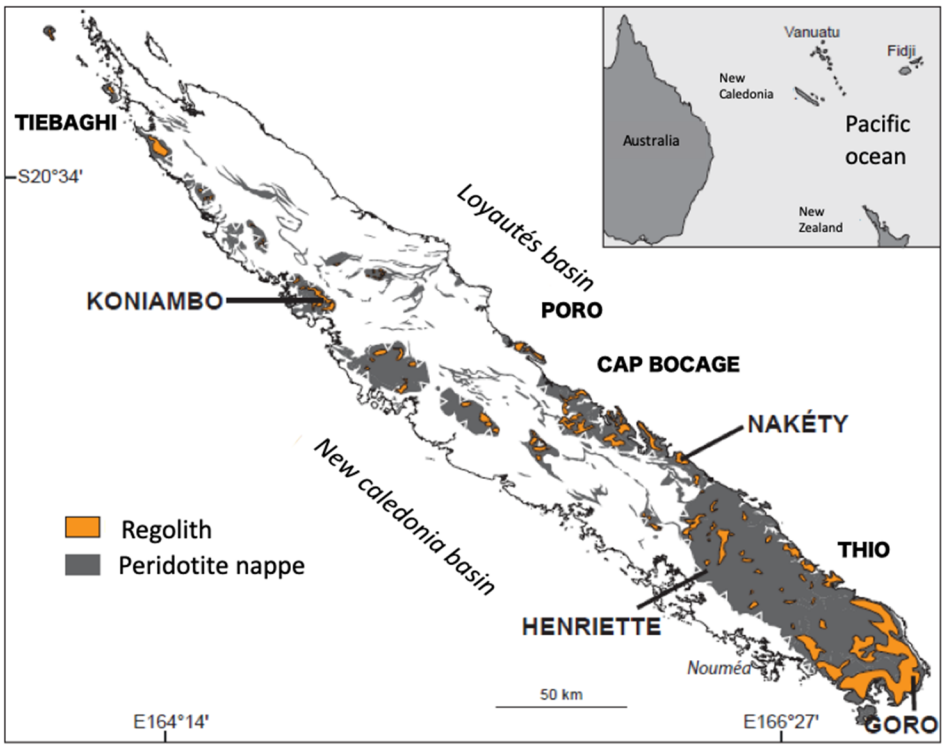

Figure 2. Geological map of New Caledonia after [31,55]. The studied deposits mentioned in the present paper are indicated.

3. Results

3.1. Paleosurfaces and Representative Landscapes

The approach is based on the morpho-climatic sequence defined by [49], and investigates the local layering of armoured surfaces and the successions of mechanical erosion and weathering phases. Observations can be generalised through the proposed regional correlation based on altitude ranges/similarities in shape and weathering. The sequence, however, is poorly constrained chronologically due to the limited availability of absolute chronological data, which are relatively scattered across the scale of New Caledonia [33,34,36]. Some of the oldest surfaces were dated around 25 Ma in Tiébaghi [36], indicating lateritic weathering since at least the Late Oligocene.

Similarities were observed at all the sites, namely the layering of relics of successive lateritic paleo-surfaces (Figure 3). The identified surfaces are primarily S1, S2 and S3. Variations in elevation difference between these surfaces indicate different incision rates. At Koniambo, S1 is around 800 m altitude, as at Opoué. It is less at Thio.

The Goro deposit exhibits the least incision, while the deposits in the Tontouta Valley area (Henriette-Opoué sites) are the most incised. In mining terminology, the latter are classified as slope-type deposits, whereas the Goro deposit is characteristic of the basin type. Despite these typological distinctions, no significant differences exist in the alteration processes and terms present across all sites. For example, the geometry of the base of the egg-box alteration profile at Nakéty is also found at Goro and Koniambo, both in outcrop and test pits. This type of heterogeneity was also noted at Opoué.

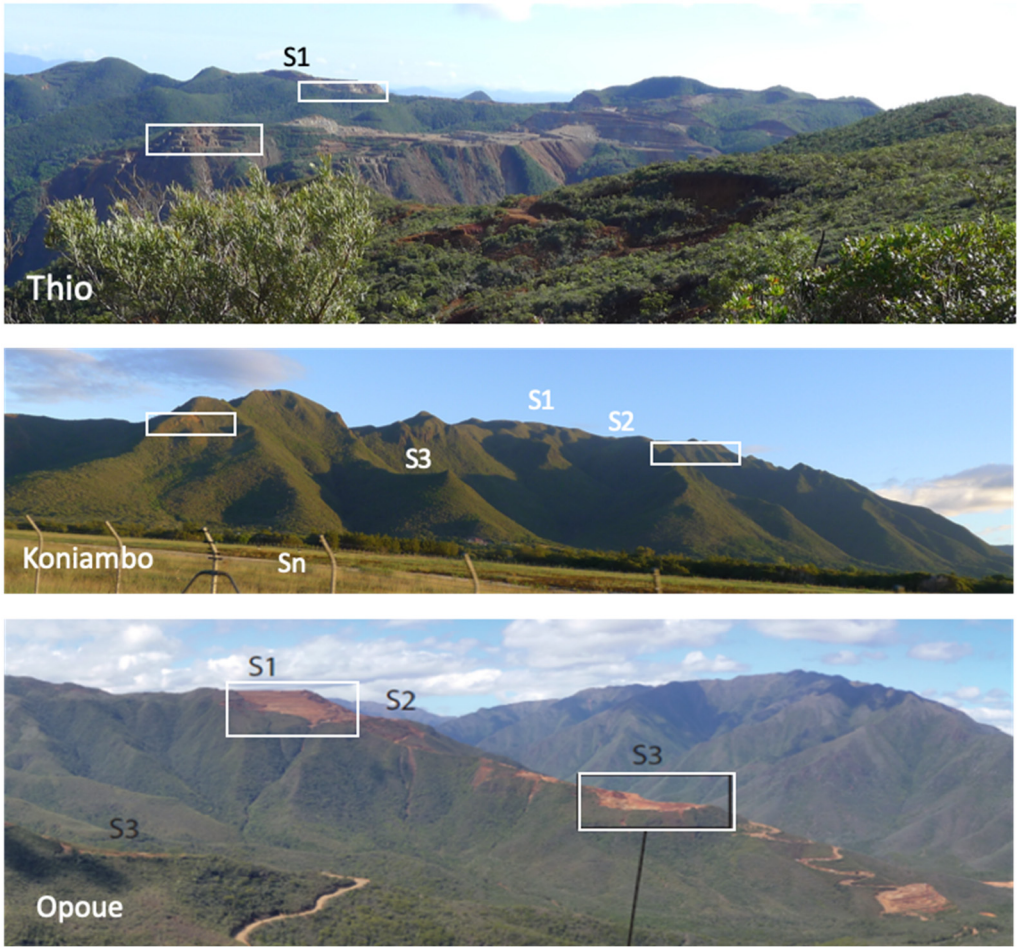

Figure 3. Three panoramic landscapes with the indication of paleosurfaces (S1 to Sn; as defined elsewhere by [30]) and, in white boxes, indication of the Ni-enrichment zones mined in open pits.

These sites, therefore, have shared histories linked to the chronology of the surfaces, which involves the entire island. The differences in geomorphological history will impact the geometry of the deposits, influencing whether there is lateral continuity between the weathering profiles and the extent to which karstic systems are marked depending on the incision rate [14].

In the case of Goro (Grimaud et al., submitted), the weathering profile is thick—particularly the lateritic part—which is commonly 30–40 m thick and can reach up to 55 m locally. We suggest that this high thickness may be linked to the low incision rate in the landscape. The weathering profile of stage S2 is reactivated during the subsequent weathering phase associated with stage S3. This hypothesis is supported by the observation that the thickening of the weathering profile coincides with the limit of the S2 surface towards the S3 surface (Figure 4).

3.2. Ore Types

Field observations at the various study sites highlighted and confirmed the role of pre-existing serpentine fracturing in facilitating chemical weathering. The impact of fracturing differs according to the nature and orientation of the fractures and the local geomorphological context. It is more significant in deposits on slopes or dissected plateaus. Subvertical fractures or fractures oriented parallel to the topographic slope— i.e., in the direction of drainage on a hectometric scale—appear conducive. They increased drainage and, hence, chemical alteration.

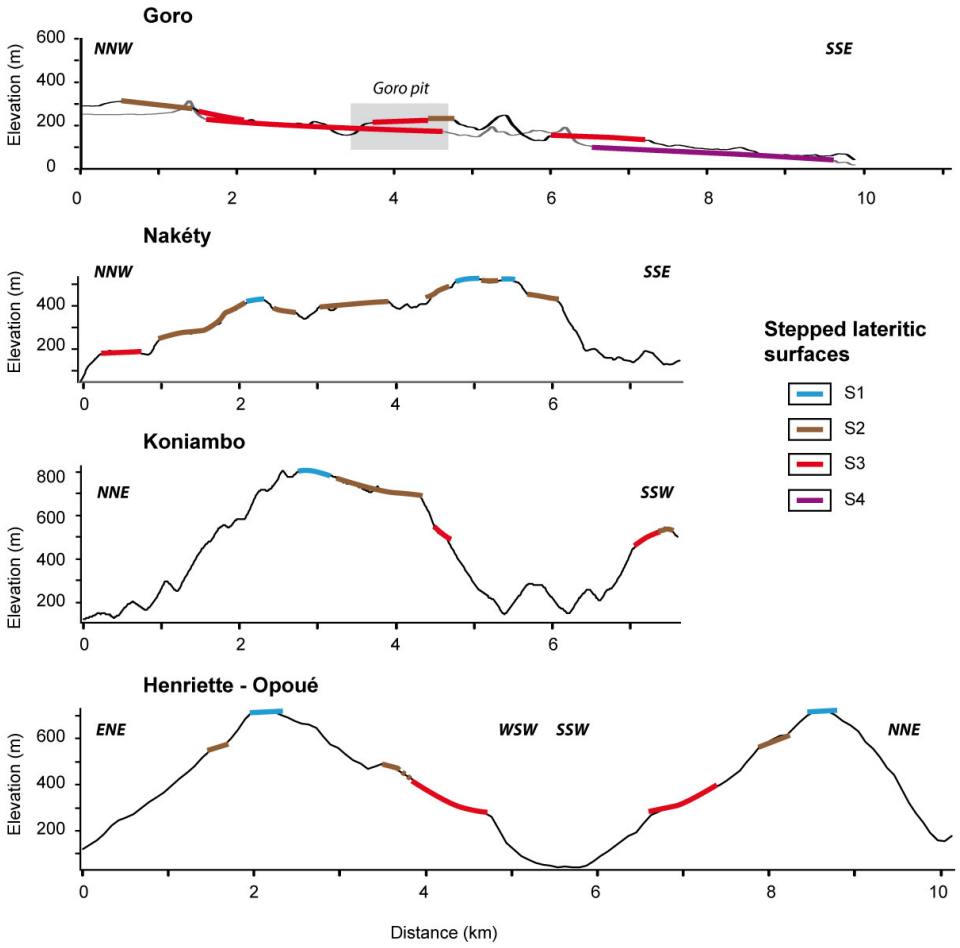

Figure 4. Distribution of paleo-surfaces (S1 to Sn) in found typical profiles: slope-dominated profile (Henriette-Opoué; plateau type (Koniambo); flat low latitude plateau (Nakéty); basin type (Goro).

On the contrary, fractures with a shallow gradient, generally controlled by the "magmatic" bedding and oriented opposite to the hydraulic gradients, are only slightly reactivated by supergene processes. They act as barriers to alteration development, particularly when filled with serpentine. At Henriette, the emplacement of slipped masses was promoted by fractures oriented perpendicular (but dipping towards) to the slope. In addition to their role in chemical alteration, major serpentine faults parallel to the direction of underlying valleys can also favour the emplacement of slipped masses, as observed at the Henriette site.

The geometry of the inherited fracture network is an important parameter to consider. However, the re-opening of these structures occurs during several stages, reflecting a multistage evolution of the fracture system over time: (i) syntectonic stages correspond to compressive stages [46,56]; it occurred probably at a deep structural level, as the temperature of the fracture infilling is interpreted from isotopic data obtained on microcrystalline quartz around 70 °C [19]; (ii) normal faults correspond to later stages and are associated with more surficial water–rock interactions following exhumation [35,57].

3.2.1. Syntectonic Ni-Talc-like Veins

Cathelineau et al. [18,19] described a succession of crack-seal episodes associated with specific mineral assemblages at the Koniambo mine site. Similar crack-seal mineral assemblages were found across all studied sites in New Caledonia [56]. Figure 3 illustrates the earliest fracture-filling assemblages from several sites other than Koniambo.

At Koniambo, type 1 ore consists of veins sealed by fissures that exhibit a succession of fills, beginning with Mg-Ni talc-like, followed by red microcrystalline quartz impregnated

by iron oxide micro-inclusions. Talc-like phases are enriched in nickel within the range of 5–20% NiO and typically develop onto the lizardite/polygonal serpentine from older fractures after reopening. These mineral fillings are linked to tectonic events that enabled the circulation of reduced fluids at low temperatures (50–70 °C) and the mixing with oxidising waters. This process likely occurred at a greater depth than the current level, between the bedrock and the yellow lateritic horizon.

Figure 5 highlights the similarity of fractures filled with talc-like from ore stage 1 across multiple sites in New Caledonia. Most fractures were initially filled before the obduction of the peridotite nappe by lizardite ± magnetite synchronous with the hydration of the mantle wedge. The lizardite fractures formed during obduction are sometimes converted into light-green polygonal serpentine. These fractures were reopened and filled in a crack seal process, first by blueish-green talc-like and then by micro-crystalline red or hyaline quartz.

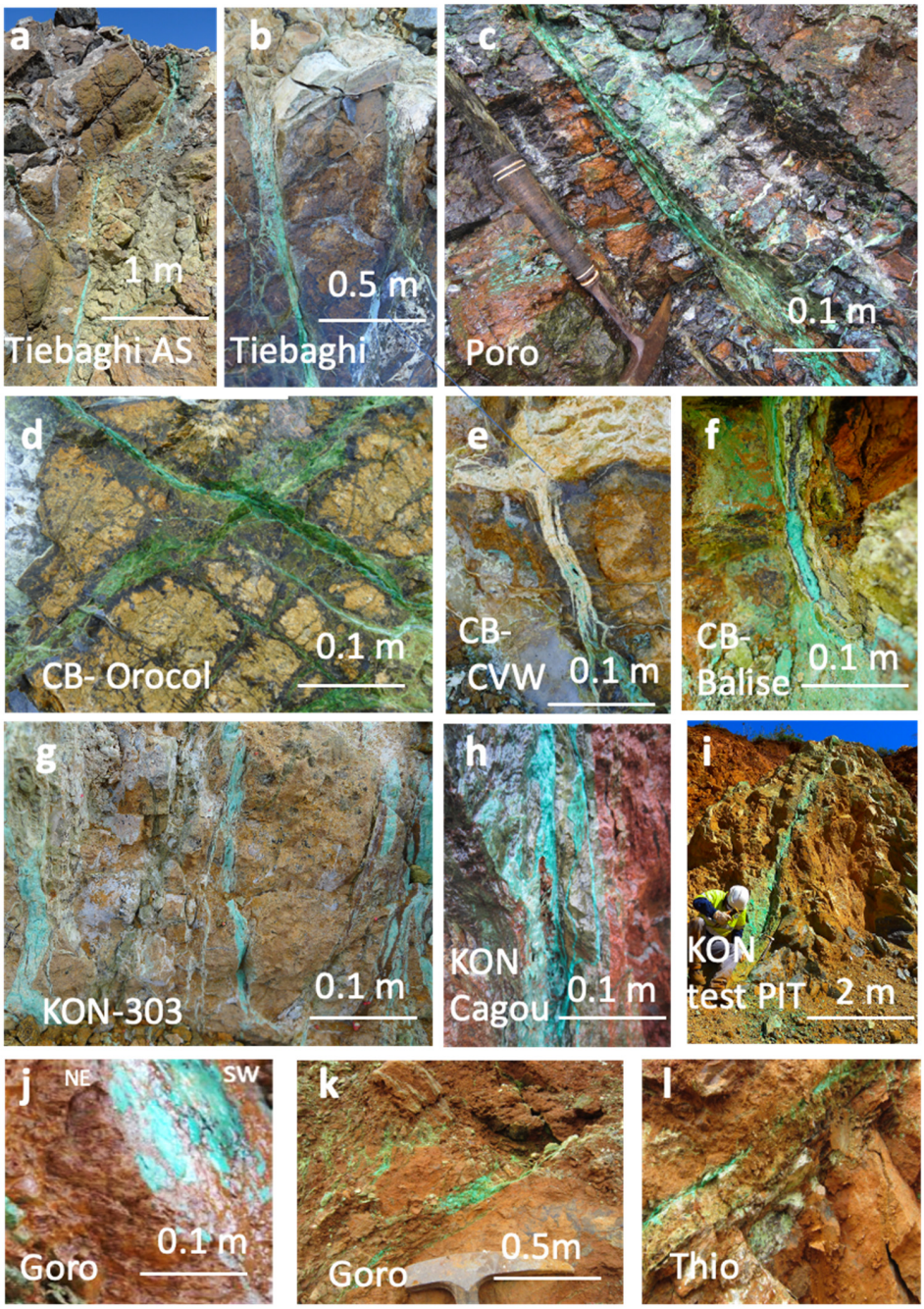

Figure 5. Representative examples of syntectonic ores and talc-like fissures are Tiebaghi, Poro, Cap Bocage (CB with different ope pits: CVW, Orocol, Balise), Koniambo (KON, open pit Cagou), and Goro.

3.2.2. Ni-Cockade Ores and Pimelite-Breccia

Type 2a ore formed later, closer to the surface, through evaporation within joints developed in metric-sized boulders. This ore type consists of films with concentric zones of pimelite (Ni-rich end-member of the Mg-Ni talc-like series) at the periphery and Mg-talc-like at the centre ([19] for the Koniambo site). Similar cockade ores were identified at most other sites (Figure 6), except Goro, where examining early ores is complicated by the deep penetration of the oxidation, where most silicates are dissolved.

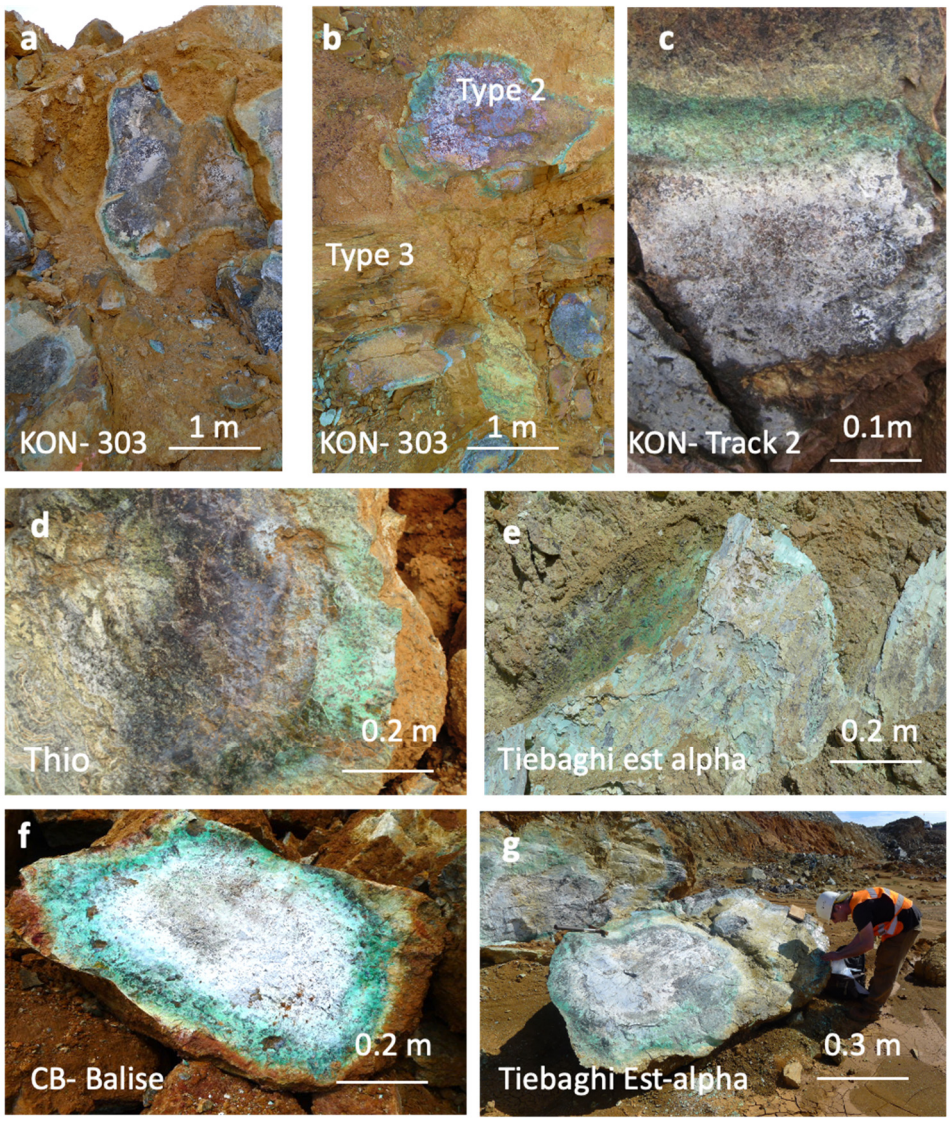

Figure 6. Representative examples of cockade (target-like) ores consist of films of talc-like (Mg-talc-like is whitish in the middle, and the green domain at the periphery of the fracture is filled by Ni-talc-like with a composition close to pimelite. These films are interpreted as being formed by evaporation in fractures crosscutting large boulders. Examples from: (**a**,**b**) Koniambo (Open Pit 303); (**c**) Koniambo, along Track 2; (**d**) Thio deposit; (**e**,**g**) Open Pit "Est Alpha" from Tiebaghi; (**f**) Open pit "Balise" at Cap Bocage.

The breccia with pimelite cement (ore type 2b) has been described by [14]. The type locality for this ore type is the "Cagou" open pit at Koniambo. A karst conduit developed along a primary fracture and collapsed, forming a breccia pipe. Dark-green pimelite and white quartz cement the collapsed breccia fragments. The karst systems associated with these structures can reach deep levels, extending a few hundred meters below the surface [58].

3.2.3. Ferruginous Saprolite Ores Dominated by Silicates

The ores currently mined (type 3) have formed due to the deepening of the silicate dissolution front. This process affects all the previous mineral assemblages and redistributes the nickel in a complex fine-grained mineral assemblage of serpentine, talc (±nontronite) and goethite distributed around the boulders (Figure 7). This saprolitic horizon forms a fine-grained metric to decametric layer surrounding the preserved boulders.

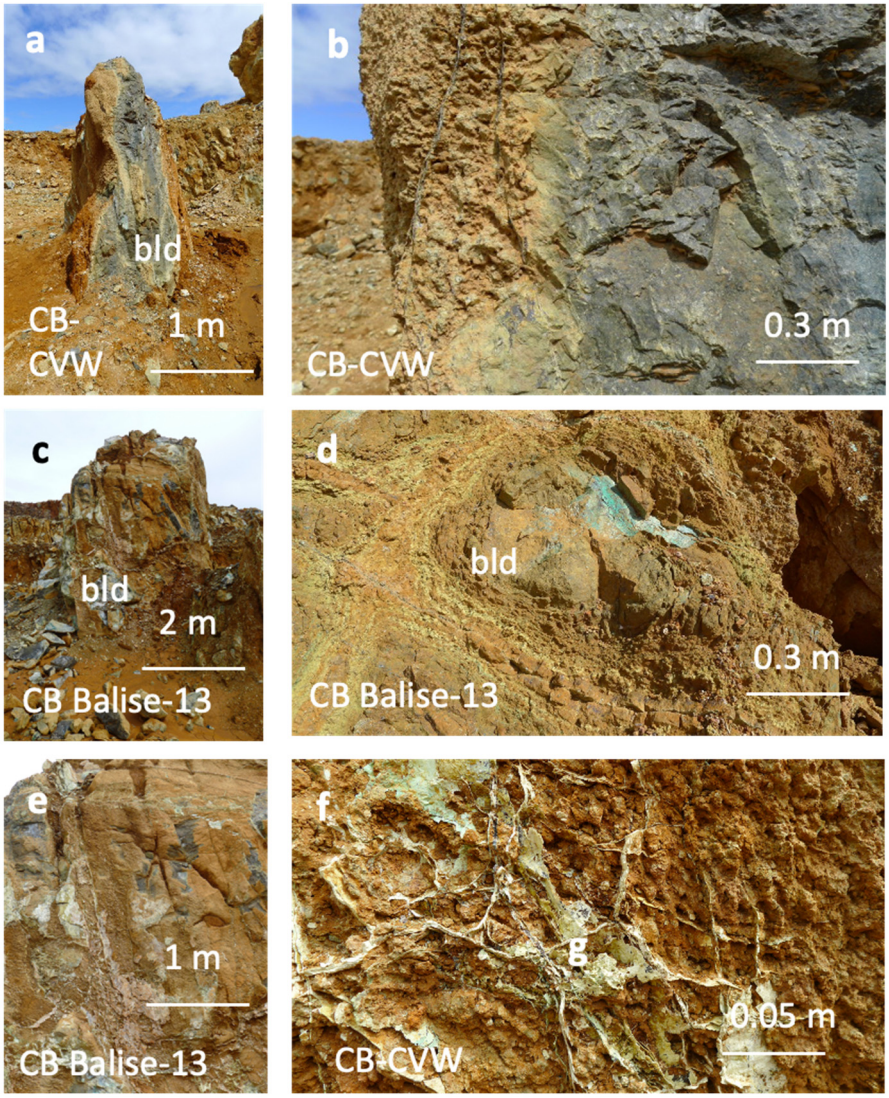

Figure 7. Representative examples of type 3 ores exploited today on the example of the Cap Bocage open pits (CVW and Balise-13). Relics from stage 1 and 2 ores partially to almost completely dissolved mineral assemblages are still visible within the fine-grained ore type 3 composed of silicates, inherited serpentines, talc-like ± nontronite, and goethite. (**a**): Boulder (bld) left behind by quarry machinery because not usable as ore in pyrometallurgy; (**b**): detail of the boulder margin, generally enriched in nickel in microfractures; (**c**): huge isolated boulder; (**d**): advanced alteration with small size boulder and relics of previous Ni-rich talc-like fissures under dissolution; (**e**): bedrock showing the starting dissolution and replacement around fractures, isolating boulders; (**f**): relics of a talc-like network under dissolution in the saprolite.

The saprolite thickness varies from a few decimetres to several decametres. Ni-enrichments characterise the middle part of the saprolite. Above the boulders, only relics of ore types 1 and 2 are observed, but enrichments are systematically observed at the periphery of the boulders. The saprolite is fine-grained and has a low rock density, as textures are generally preserved despite extensive dissolution of mantle minerals. The

boulder surface is often highly irregular, as illustrated by the Cap Bocage mining site (Figure 7). By comparison, the topographic surface of each paleo-landsurface, located 20 to 50 m above the boulders, is smoother.

3.3. Geochemical Evolution Along Laterite Profiles

Figure 8a shows a typical oxide-rich lateritic geochemical profile across the laterite in the example of Goro. The rocky (sap-rock) to earthy saprolite interface constitutes the most prominent geochemical transition with the sharp depletion of SiO_2 and MgO from 40 to <5–10 wt%, and the concomitant increase in Fe_2O_3 from ~4 to ~60 wt%. From the base of the earthy saprolite up to the ferricrete, Fe_2O_3 concentrations increase up to ~70 wt% together with a further decrease of the SiO_2 and MgO contents. Divalent elements, such as Mn, Ni, and Co, exhibit a tenfold enrichment in the lateritic profile compared to the parent peridotite. However, most of these elements display different distribution patterns than Fe in that their maximum concentrations occur at intermediate positions within the lateritic profile. Ni usually reaches maximum concentrations in the rocky saprolite (~2 wt%) and almost linearly decreases in concentration upwards in the profile. Similarly, Mn and Co concentrations are maximum at the summit of the earthy saprolite and decrease upwards in the yellow laterite. Trivalent elements are at their maximum in the yellow limonite.

The evolutions are summarised in the triangular diagram Mg+ Ni/Fe+Al+ Cr/Si (molar), which shows a significant decrease of Mg towards the Si-Fe+ Al+ Cr line and the progressive decrease in Si in the saprolite down to a few % in the yellow and red limonite.

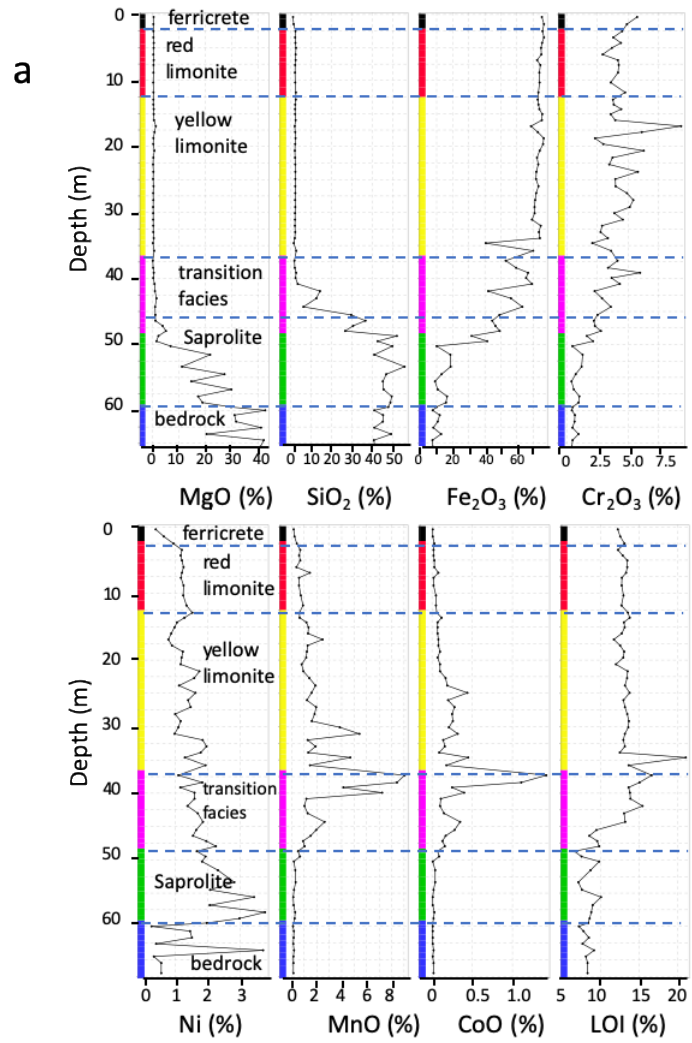

Figure 8. *Cont.*

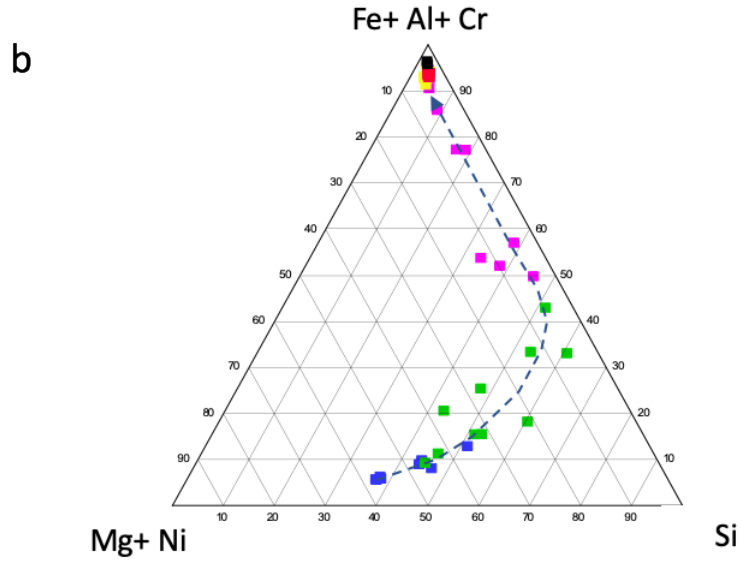

Figure 8. (**a**): Geochemical evolution along dunite-derived laterite profile at Goro: (**a**) Major oxides: MgO, SiO_2, Fe_2O_3, Cr_2O_3, and: Ni (pct = wt%), MnO (%) CoO (%) and Loss of Ignition (LOI, %). (**b**): Triangular diagram Mg+ Ni/Fe+Al+ Cr/Si (molar) for the same profile. Square colors correspond to colors for each horizon from Figure 8a. The dashed line and arrow provide the sense of the evolution from unaltered bedrock to the upper laterite horizon (ferricrete).

3.4. Detailed Mineralogy

Silicate nickel ores, which can be processed by pyrometallurgy, are located between two primary interfaces: the bedrock-saprolite interface and, above, the saprolite-yellow laterite interface.

Micro-XRF chemical maps of Fe, Cr, Ni, and Mg provide a good picture of the micro-fracture network and their fillings across different scales. Chromites underline the magmatic layering, while Ni is predominantly concentrated in fractures at all scales. In contrast, Si, Mg, and Fe are more dominant within the matrix (Figure 9).

At the bedrock interface, following the dissolution of olivine (±pyroxene), the fluids re-saturate with nickel silicates (serpentine and talc in New Caledonia [14,18,19] and in Indonesia [59]), talc and especially sepiolite in the Dominican Republic and Cuba [20]. In New Caledonia, these nickel silicates precipitate, as shown by the results of the CNRT Transnum project, most often in a network of thin and dense pre-existing micro-fissures probably pre-obduction [47]. Talc-like also occurs along the network filled by lizardite formed in a late stage of peridotite obduction, mainly in a brittle regime and developing a network of discontinuities on all scales [46]. Above the saprolite within the yellow or red laterite, silicates have mostly disappeared due to dissolution, leaving only hydroxides and oxides (predominantly iron and occasionally aluminium).

Two distinct zones can be distinguished (Figure 9c,d). The saprock zone is enriched in Fe at the expense of Mg compared to the least altered rock. In addition, the apparent density of Ni-bearing fractures is higher in the saprock zone (Figure 9e,f). Ni is present in the major and secondary fracture networks within this zone.

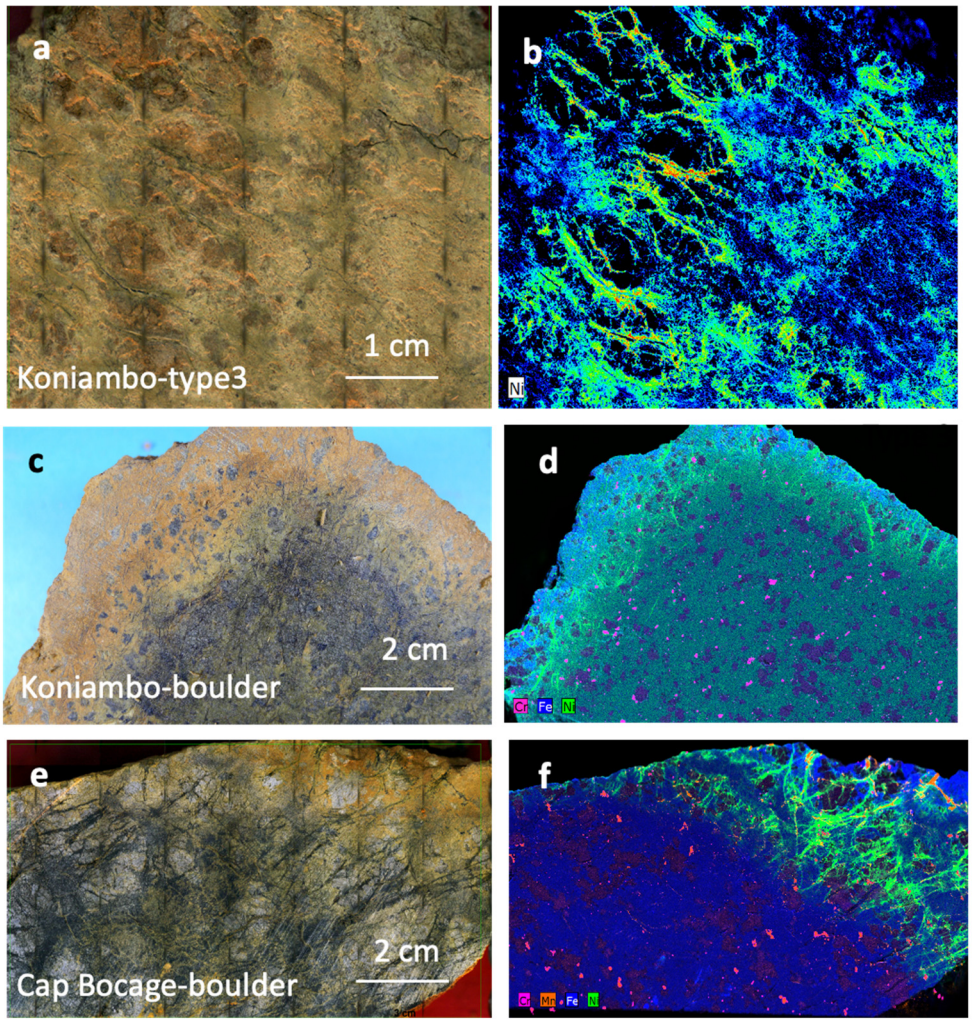

Figure 9. Representative examples of macroscopic features of type 3 ores and the related distribution of metal enrichments (Ni, (Fe, Mn, Cr) distribution in micro-XRF composite maps) around boulders. (**a**,**b**): Fine-grained type 3 ore constituted of silicates impregnated by iron hydroxide with a complex distribution of nickel mainly enriched along pre-existing micro-fissures; (**c**,**d**): boulder with enrichment in nickel at its periphery (in agreement with XRF analysis of a boulder section in [22]); (**e**,**f**): detail of the peripheric Ni -enrichment around the boulder, within the pre-existing lizardite network appearing in black fissures (**e**), and green (**f**).

3.4.1. Recommended Characterisation Methodology

Characterisation of the distribution and nature of Ni, Co, and Sc carriers can be carried out by combining:

- Macroscopic approaches include direct observation and chemical mapping using micro-XRF on samples as large as 20 centimetres. These methods are complemented by detailed mineralogical characterisation of representative quartered samples from ore bags (global approach using XRD and quantitative chemical analysis). A challenge in this approach is correlating the overall chemical characteristics with quantitative mineralogy, especially in cases where a mixture of yellow-to-red laterite and cork-type ore lacks discernible mineralisation. Using Rietveld-type methods for quantification, XRD can be employed for this purpose.
- In situ approaches focus on samples selected based on observational criteria characterising the distinct mineralogical assemblages. Although this sampling method targets typical assemblages, it does not represent the ore heap as a whole. Instead, it provides

insights into the characteristic assemblages without quantifying their contribution to the overall chemical and mineralogical properties.

It should be noted that micro-phases have to be observed at different scales ranging from a few tens of microns (thin sections) down to a few tens of nanometres (scanning electron microscopy and transmission microscopy) due to the tiny size of the main carriers (except "garnierite" micro-veinlets). Quantitative in situ chemical analyses by electron microprobe and SEM-EDS cover around 1 to some cubic microns and are very often mixtures (e.g., serpentine + talc), whereas analyses carried out by TEM are generally semi-quantitative (and obtained by correcting the raw analyses with K-factors calibrated on standards) but allow for approximating the chemical characteristics of the carrier phases at a nanometric scale.

Additionally, an in-depth mineralogical study can be carried out using X-Ray absorption spectroscopy to identify the direct atomic environment of the element of interest. Typically, two distinct approaches can be applied. The first consists of measuring X-Ray absorption spectra on bulk samples, using a wide X-Ray beam (>mm), reduced to powder and homogenised, to deduce the average speciation of the photo-absorber metal in the bulk rock. The second involves in situ measurements using a micro-focused X-Ray beam (<µm), enabling localised identification at the scale of individual mineral phases to identify the associated speciation modes of the photo-absorber metal.

3.4.2. Mineralogical Characterisation

The advance of the mantle silicate dissolution front (forsterite, enstatite) is marked by increased porosity but does not affect the serpentine network within which Ni becomes concentrated. Electron Probe Micro Analysis (EPMA) shows the heterogeneous and moderate Ni-enrichment in the inherited serpentine network ranging from 0.4 to around 7 wt% Ni. Such heterogeneities appear to be partly inherited from the nature and crystallinity of the serpentines. Finally, although congruent dissolution of mantle silicates remains dominant during the saprolitisation of peridotites, incongruent dissolution processes are also locally observed, with silicates replaced by quartz and tri-octahedral smectites (nontronites). Iron- and nickel-bearing nontronites can be found either in a multi-meter layer (as in the case of Tiébaghi in New Caledonia, or, more often, as a discrete replacement of mantle minerals (as observed across all investigated sites). The smectites identified generally contain 1 to 4 wt% Ni, so the olivine conversion in smectite does not affect the overall Ni content of the saprolite ore.

EPMA of the serpentine veins in saprolitic ores commonly exhibits an apparent chemical transition from the serpentine pole to the talc-like pole (Figure 10). The moderate Ni enrichment observed in serpentines may be associated with an increased presence of "talc-like" sheets at a scale smaller than the micron-sized volume analysed with EPMA. This process would be more complex than a simple mechanical mixing between a Fe-free kerolite similar to those developed in crack-seals and a Fe-bearing lizardite. Assuming that iron is absent from talc-like particles, its concentration should decrease as the proportion of talc-like particles, and therefore the Ni content, increases. However, the iron content remains sub-constant in most analysis points, indicating a more nuanced interaction.

The nature of nickel carriers within saprolite, explicitly distinguishing between serpentine and talc-like minerals, was further examined using Transmission Electron Microscopy (TEM) (Figure 11). These TEM studies revealed that nickel-bearing talcs can form distant from any kerolite-bearing veins by epitaxial growth on pre-existing serpentine sheets within the microcrack network at the periphery of boulders [14]. At this stage, no nickel-bearing serpentines appear to form; however, serpentines often display significant nickel content, up to about 7 wt% NiO, without evidence of talc presence, suggesting a serpentine transformation with moderate nickel incorporation. No nickel mineralisation in New Caledonia is directly supported by "nepouite"-type serpentines (the nickel-rich end member of lizardite). Instead, talc-(like) and Ni-enriched serpentine are the primary carriers. These nickel-bearing talcs are characterised by a few stacked sheets and small sizes, in the order of a hundred nanometres, making mechanical separation and pre-enrichment nearly impossible.

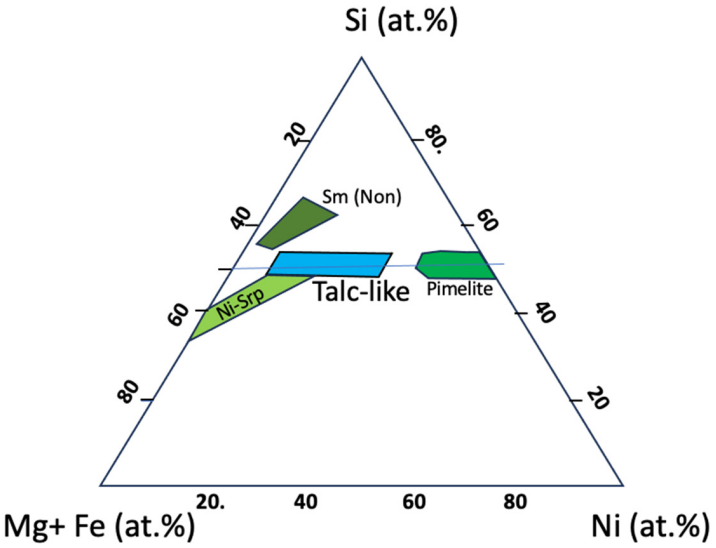

Figure 10. Main Ni-mineral phases found in saprolites from New Caledonia, and the ore types: in blue, talc-like found in ore type 1 and saprolites; in light green, serpentine (Ni-Srp) enriched in nickel from the microfissure networks found around boulders, pimelite from breccia (type 2b breccia ores, and target like ore type 2a, Koniambo), and late fractures (Poro example). Tri-octahedral smectites (Sm) (Fe- nontronites, example of Tiébaghi).

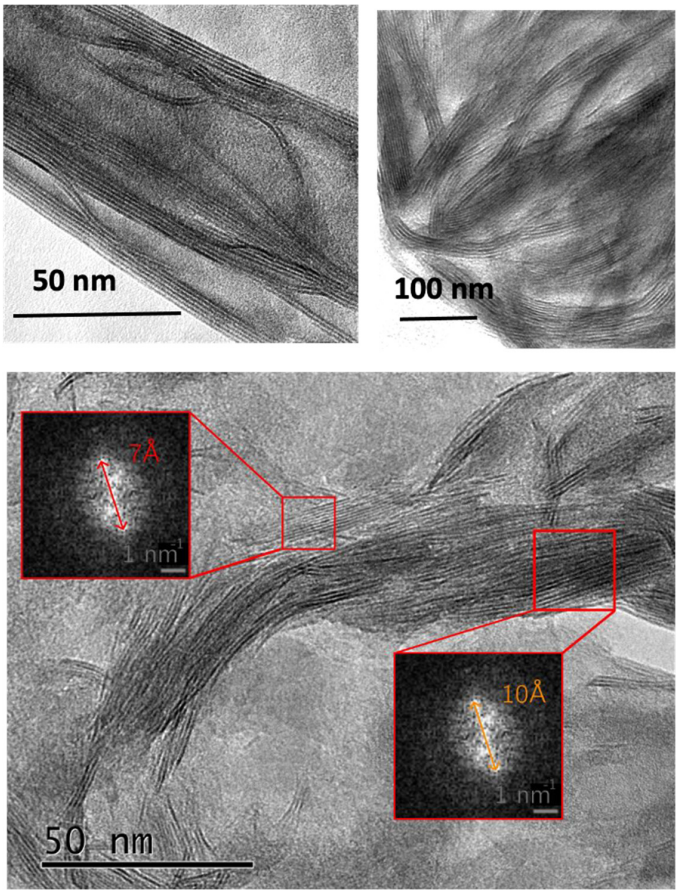

Figure 11. Main Ni-bearing mineral phase in ores from stage 1 to 3 observed under HR-TEM: talc-like from the blueish-green veins from stage 1; talc-like from pimelite ores in karst breccia (ore type 2); talc-like from ore type 3 (ferruginous saprolite). The talc-like are again found within the original serpentine framework inherited from the obduction stage. The talc-like are crystallised onto the serpentine layers at the nanometric scale.

This study directly observed two types of nickel enrichment within facies distal to garnierite veins. These enrichments are linked to:

(1) Talc-like precipitation within the serpentine network. These talc-like deposits are, to some extent, similar to those already described by [14,19] in most of the "garnierite" mineralised veins (Tiébaghi, Koniambo, Poro, Thio, Népoui, Cap Bocage, Henriette, Goro). The TOT talc-like structures may constitute a significant Ni-bearer and are much richer in nickel and silicon than the serpentines (TO).

(2) Moderate nickel substitutions in lizardites within their crystal lattice. Ni-bearing serpentines do not correspond to nepouite, as reported in earlier work. Nepouite has never been found in the samples studied over the last ten years. However, serpentines can be moderately enriched in Ni up to a few per cent NiO (e.g., [22]). These in situ investigations constitute the first direct observations of saprolite ore without macroscopically observable nickel-bearing phyllosilicates, where nickel appears enriched in inherited lizardite-type black serpentine microstructures. In agreement with our previous spectroscopic study [60], our nanometric scale observations confirm the crystallisation of fine talc-like particles localised in pre-existing serpentine networks and the incorporation of Ni in the serpentines.

3.4.3. Use of Ni K-Edge XANES Spectra for Determination of Ni-Bearers in Bulk Rock

Linear combination analysis of the XANES (X-Ray absorption near edge structure) spectra collected from the Ni K-edge can identify and quantify the main nickel-bearing phase in the total rock. To do this, XANES spectra must first be measured for each potential nickel-bearing phase using the database already published by [22]. In the latter study, µ-XANES spectra were collected on a mineralised, multiphase vein in the Koniambo massif, including oceanic lizardite (mesh and weathered lizardite), neo-formed lizardite, polygonal serpentine, and talc-like with different Ni concentrations (Figure 12a). To assess the main Ni-bearing phase in the main Ni-bearing lateritic horizon; i.e., the saprock horizon, a linear combination fit (LCF) is performed on the bulk XANES spectrum (see red dashed line in Figure 12b). The results clearly show a mixture of two speciation modes for nickel, with a proportion of 65 mol% polygonal serpentine and 35 mol% talc-like. However, these latter phases contain around 5 and 36 wt% NiO, respectively. As a result, 95% of nickel in the sap-rock horizon is hosted by polygonal serpentine, whereas only 5% of nickel is hosted by the more concentrated phase; namely, the talc-like phase [60]. This result cannot be generalised, but it confirms the observations carried out by TEM about the mixing at the nanoscale of the talc-like and Ni-contaminated serpentine. At a larger scale, microprobe data also show the mixing trend between serpentine and talc-like (Figure 10).

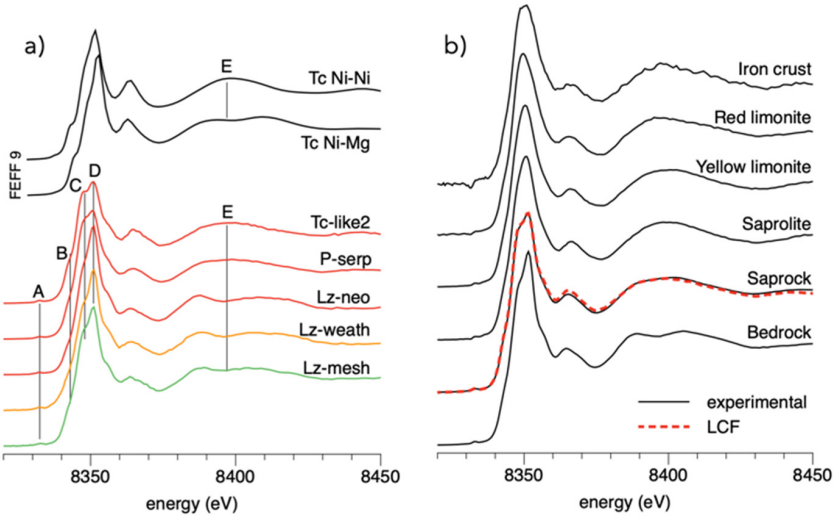

Figure 12. (**a**) µ-XANES spectra obtained at the Ni K-edge for different nickel mineralised veins in a saprock facies boulder from the Koniambo massif. Note that the two black spectra on top of the graphic

result from ab initio calculation help us understand the meaning of feature E, indicating the presence of either Ni-Mg bonding or Ni-Ni bonding (i.e., Ni clustering; from [22]); (**b**) series of XANES collected on bulk rocks (large X-Ray beam), on different horizons of the Koniambo lateritic profile. LCF is only performed on the spectra from saprock, matching with a mixture of Ni-bearing polygonal serpentine and Ni-bearing talc-like. Note that the bedrock matches with oceanic lizardite, and spectra from the upper parts of the profile require Ni-bearing oxi-hydroxide model compounds, as shown in [21].

4. Discussion

4.1. Role of Micro-Fractures in Ni Redistribution During the Bedrock-Saprolite Transition

The coupling of the micro-structural geometry with chemical imaging of the alteration front's progression guided by the micro-fracture network has led to the following conclusions:

- Micro-fracturing is a preferential network controlling the transfer and mobility of Ni-Mg-Si and their re-precipitation as newly formed minerals.
- Inherited serpentine fillings play a crucial role in the epitaxial or topotactic precipitation of nickel in the form of Ni-Mg talc on the surfaces of pre-existing serpentines. The serpentines are primarily lizardites, which may be partially replaced or transformed into polygonal serpentine.
- The combined role of: (i) micro-fracturing (micro-structural heritage linked to the initial functioning of the serpentinisation networks or their reactivation under crack-seal conditions (stage I of Ni-Mg talc mineralisation then micro-crystalline red quartz) or reopening by surface bursting; (ii) the mineral inheritance linked to the presence of two types of serpentine along the microcracks, during the reopening phases of these networks is effectively visualised by the micro-XRF maps of nickel, iron, silicon and magnesium.

4.2. Role of Macro-Fractures on the Morphology of the Bedrock-Saprolite Interface

Development of the Boulder and Saprolite

The peridotite massifs of New Caledonia exhibit intense fracturing, which plays a crucial role in controlling the permeability of these environments. At the deposit scale, the progression and geometry of the alteration front are primarily governed by fracturing. Zones align with areas of weakness, typically associated with damaged and micro-fractured regions adjacent to wider serpentine-filled fractures. Nickel-bearing fractures mirror the prominent structures at the outcrop and quarry scales, indicating the reactivation of inherited fractures (Figure 13). When the dissolution of olivine is almost complete, only tracks of the early fractures remain, which are underlined by relics of serpentine or talc-like. From the early distribution of nickel controlled by the microfracture lizardite network on the one hand and the major fracture and faults on the other to its distribution in the saprolite, there is a progressive homogenisation through dissolution and recrystallisation. New mineral phases bearing nickel occur, such as goethite or nontronite locally, which are mixed with relics of the early Ni-bearers (Figure 13). Ore type 3 in Figure 13 is the resulting association and forms ores such as so-called "minerai bouchon" by miners; e.g., a low-density rock (frequently lower than 1), with a colour close to cork.

The similarity of redistribution processes across different scales can be attributed to structural control and scaling laws that determine the distribution, orientation and size of discontinuities. The fractal nature of the fracturing networks accounts for the structural organisation observed across all scales.

The alteration front and nickel redistribution progression model is consistent from the sample to the outcrop scale. The roughness of the saprolite-bedrock interface is controlled by a rhythmic pattern of fracture sets, which are generally well-defined with constant recurrences.

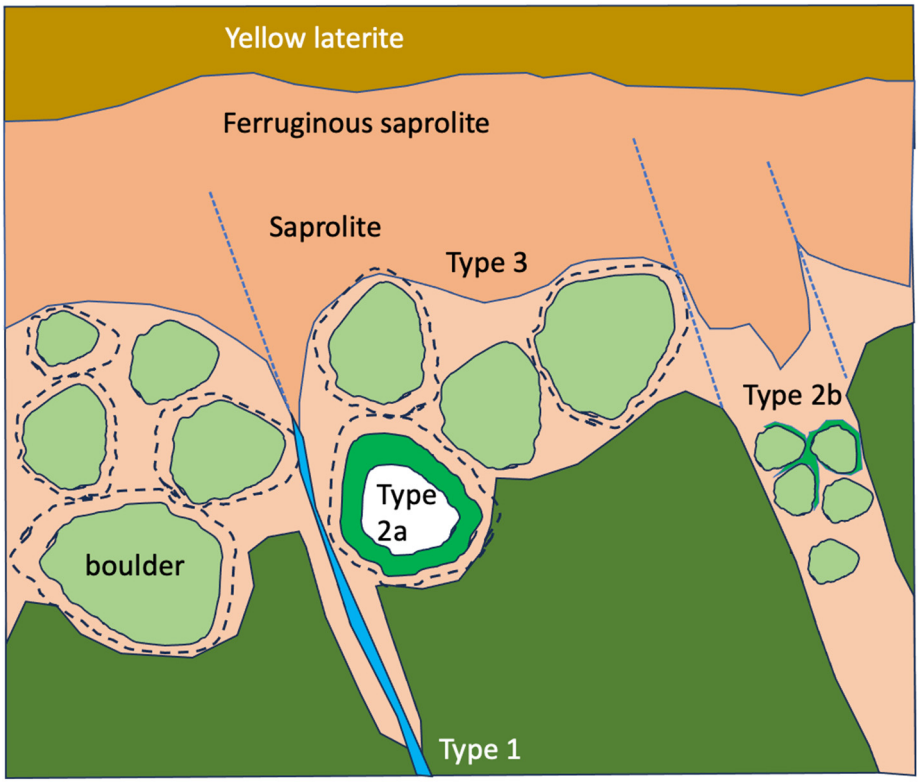

Figure 13. The main types of Ni-ores at the base of the saprolite: (i) type 1, crack-seal vein (blueish talc-like) developed along serpentine fractures; (ii) type 2a, target-like coating crosscutting a boulder; type 2b, pimelite-quartz infillings of karst breccia; (iii) type 3 ore, saprolite containing fine-grained ore (talc-like and Ni-enriched serpentine), associated with nontronite in some deposits.

4.3. Chronology of the Formation of Paleosurface and Development of Boulders

Despite the typological distinctions between the different deposits, there are no significant differences in the processes and types of alteration present on all the sites. Layers of relics of successive lateritic paleo-surfaces are found at most studied locations. The surfaces associated with mineralisation are mainly S1, S2 and S3.

Differences in geomorphological history significantly influence the geometry of the deposits, particularly in terms of the lateral continuity between the alteration profiles and the impact of karstic systems, which vary according to incision rates. Consequently, differences in altitude and local incision regime mainly control the typology of the sites, influencing the relative thickness of the different horizons of the laterite profiles.

The different levels of these surfaces indicate varying incision speeds. In the Tontouta Valley area (Henriette-Opoué sites), the profiles are highly incised, with the deposits occurring on slopes. Similarly, at Koniambo, the incision between S2 and S3 explains the continuity of karst sinking. During the S2–S3 event, quartz cemented the karst breccia. The low negative δ^{30}Si values of quartz, ranging from −5‰ to −7‰, are typical of silcretes [14]. This event could correspond to a drier climatic episode than the usual tropical climates of the Eocene–Oligocene as it presents similarities with the development of Australian silcretes [61]. This climate change occurred during the Miocene and has been documented in Queensland and other parts of Australia [61–63].

The Goro deposit, a basin-type deposit, exhibits a minor incision, resulting in an oxide-dominated laterite profile up to 30–40 m thick and locally reaching 55 m thick. We suggest that this substantial thickness is directly linked to the low incision in the landscape. The weathering profile of stage S2 is reactivated during the subsequent weathering phase associated with stage S3. This inference is supported by the observation that the area of over-thickened laterite coincides with the location where the S3 surface is superimposed on the S2 surface.

In some places, such as Koniambo, a strong inversion of relief has occurred since the formation of the S2 surface [14,15]. If the paleosurfaces observed on the Koniambo plateau are synchronous with those at Tiébaghi, an age of around 25 Ma [36] could be proposed for the alteration phase of the S1–S2 surfaces. The inversion became more pronounced during the S3 surface stage and increased during the S4 stage. It was synchronous with the developing of a karst system, which led to the formation of a breccia cemented by pimelite-quartz, most likely during an arid phase during the Miocene [14]. Depending on their location in New Caledonia, the S1–S2 paleo-landsurfaces were probably uplifted by at least 200 m to more than 500 m, proportionally to valley incision that reached hundreds of metres.

Later geodynamic events introduced extensional tectonics and a series of NW-SE normal faults that reactivated pre-existing serpentine faults [29,57,64]. These faults serve as pathways for remobilising fluids, but they also create specific barriers that impede the distribution of late Ni-ores on one side of the fault [35,41,54].

An attempt to reconstruct the evolution of the paleosurfaces with time and related laterite and Ni-ore evolution is proposed in Figure 14. Four main stages are proposed: (i) with the significant exhumation of approximately 1.5 to 2 kilometres, an early weathering front developed under tropical climate when peridotites reach subsurface, (ii) Compressive tectonic stages yielded to the formation of the earliest crack-seal fractures due to the circulation of fluids deeply that heat up to 70 °C, and their subsequent mixing with more surficial fluids. At that time, the veins formed within syn-obduction lizardite and polygonal serpentine veins and fault infillings and contaminated in nickel the inherited serpentines (ore type 1), (iii) karst development driven by river incision; dissolution along faults, formation of a karst system, and subsequent cementation of joints (target-like) during episodes of drying under more arid climate, testified by the silicon isotopic values (2a). During this period, during rain periods in the year, due to increased incision of the valley, karst developed, and collapses of the open structures yield breccia, which is cemented by the same Ni-rich talc-like as in target-like (pimelite in fractures affecting boulders, ore type 2b). (iv) Potential slipping along faults occurred during extensive movements, and Ni was locally remobilised. The deepening of the laterite profile continued, leading to the dissolution of most of the previous mineral assemblages and forming the fine-grained saprolitic ores (composed of talc-like minerals, contaminated Ni-serpentine, nontronite in some cases and Ni-goethite: ore type 3).

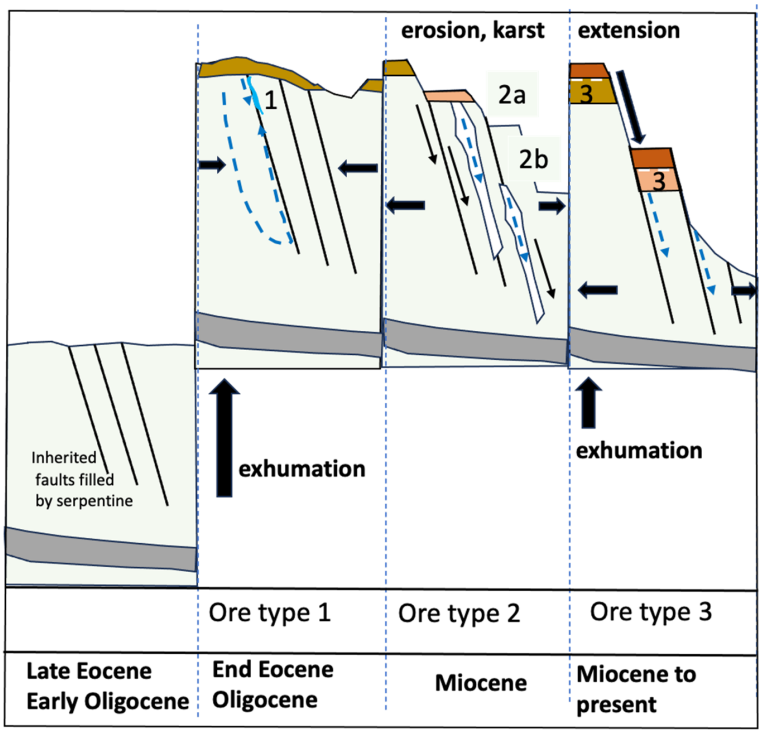

Figure 14. Evolution of plateau-type ores from Eocene to present (see text for explanations).

4.4. Modelling Reactive Transport in a Dual Permeability Environment

Several numerical models of alteration progress were developed [40,41,65]. In these models, the bedrock is fully saturated with water due to rainwater infiltration, which gradually dissolves olivine. As a result, silica, magnesium, and nickel are released, with some of these elements reprecipitating to form new minerals, including Ni- and Mg-phyllosilicates and goethite. Over time, the phyllosilicates further dissolve into goethite, giving rise to the oxide horizon. The dissolution of olivine is assumed to be kinetically controlled, while the precipitation and dissolution of newly formed minerals are supposed to be driven by thermodynamic equilibrium. For the sake of simplicity, rock porosity and permeability are kept constant, but this point will be investigated in further studies. The first modelling attempt, hereafter referred to as the 1D single-porosity (SP) model and based on a reactive multicomponent 1-D transport simulation along a porous unfractured column, revealed the vertical progression with time of the pH front, where pH stabilises around the value of 9. When olivine dissolves but remains present, the front is maintained and controls the redistribution of Si, Mg and Ni and their re-expression as Ni-silicates [40]. This process also controls the thickening of the iron-rich zone and its associated Ni enrichment.

A first 1D dual-porosity (DP) model was then developed to understand the overall impact of fractures on the alteration of peridotites [41]. An exchange coefficient drives the mass transfer between mobile regions of highly transmissive fractures and immobile areas corresponding to the rock matrix and the secondary fracture network. A comparison with existing non-fractured models highlights the control of fractures on the mineralogical speciation and alteration rates within the profile. Nickel-bearing phyllosilicates are mainly concentrated in fractures, to the detriment of the matrix dominated by magnesian phyllosilicates. In addition, fractures result in a more extensive transition zone between saprolite and laterite and, therefore, a less localised Ni enrichment than an unfractured model.

A second model, consisting of a discrete network of fractures connected to a porous matrix (DFM), was introduced to get further insight (Figure 15). This model allowed for a more detailed simulation of the complexity of alteration processes. Investigating the influence of fracture network connectivity on dissolution-precipitation processes revealed that the geometry and permeability of the fracture network significantly control the organisation of alteration zones in the matrix. By varying these two parameters, the model successfully recreated organisations typically encountered in the field, along with zones of Ni over-enrichment [41,54]. The model also successfully reproduced the formation of nickel-enriched hotspots, which are directly linked to the connectivity of the fracture network.

A comparison between the double permeability (DP) model and the single permeability (SP) model highlights the critical role of fractures in controlling alteration rates and the mineralogical distribution in the profile [41]. Including fractures in the DP model enables the recreation of Ni heterogeneities observed in the field by allowing preferential precipitation of Ni-phyllosilicates in the fractures. On the other hand, DFM modelling further captures the complexity of alteration processes by better accounting for the effect of fracture network connectivity on dissolution-precipitation processes. Works by [54] have shown that the size and geometry of boulders may be inferred from the Péclet number (Pe), a dimensionless number classically used in heat and mass transfer [66]. In this context, it represents the ratio between transfer by forced convection in fractures and transport by diffusion (within the matrix). By considering the scaling laws controlling the organisation of fracturing and its permeability, a scaling law based on the Péclet number was established to predict the minimum size of alteration heterogeneities using the hydraulic gradient across the various New Caledonian massifs. The fracture network with the highest Péclet number thus determines the spacing of the largest boulders. In addition, the width of the dissolution zone surrounding the boulder is regulated by the Damkohler number, a dimensionless number used to represent the relative importance of the reaction rate and the reactant transport by diffusion within the matrix.

The study of reactive transport at the sample scale highlights the influence of inflow and flow velocity within fractures on developing a laterite profile. A critical depth exists where

the incoming fluid must reach equilibrium with the rock before saprolitic horizons can form. This depth is a function of the flow velocity in the medium. These findings align with field observations: excessive localised flow results in pure dissolution and significant material export, preventing the fluid from reaching saturation with respect to silicates. This process explains the initial carving of preferential flow paths, leading to the formation of karsts.

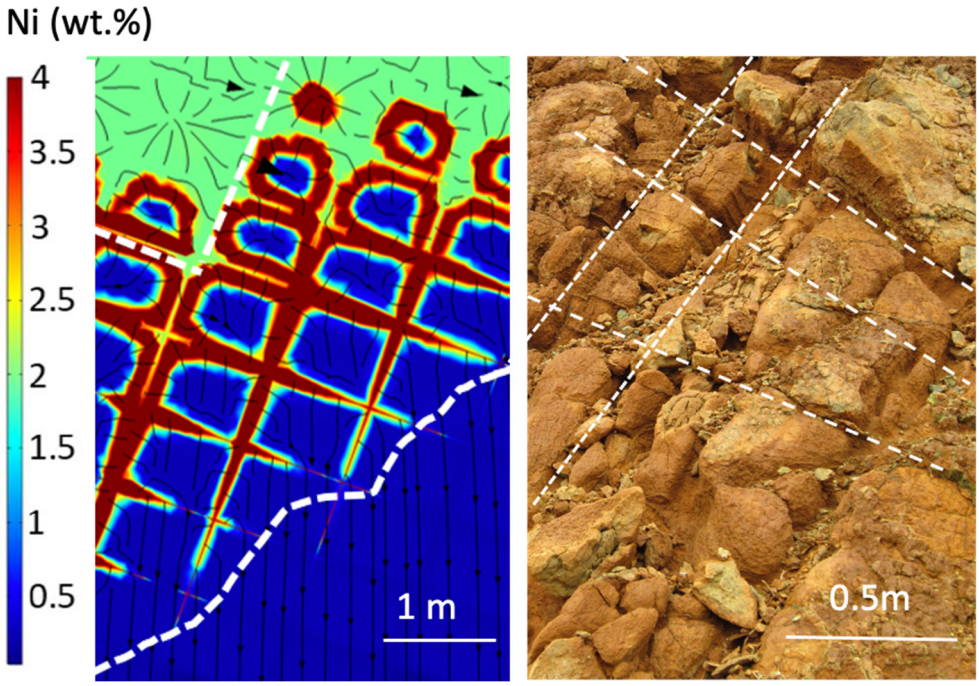

Figure 15. Modelling of the development of boulders considering the existence of two fracture systems, as they are observable in the field (example of the Thio mining open pit on the right-hand side, with main fractures marked as white dashed lines). Modelling was done using a Discrete Fracture Matrix (DFM) model at 95,000 years. (modified from [41,66]).

5. Conclusions

Conceptual models of supergene alteration in peridotite, coupled with multiscale observations of alteration and Ni-ore minerals, have highlighted the influence of inherited fracturing on the progression of fronts and the development of three distinct ore types aligned with the geodynamic and geomorphic evolution of New Caledonia.

However, identifying the exact nature of nickel-bearing phases in the fine-grained saprolite remains an analytical challenge. In combination with previous micromapping using both electron microprobe and micro-XRF, and TEM observations, advanced techniques such as XANES and EXAFS spectroscopy could help in identifying the phases and close atomic neighbours of nickel in the complex nanophases, whatever their nature: talc-like or modified serpentines.

From a geochemical perspective, there are likely numerous untapped areas for further research in lateritic soils, utilising innovative approaches developed elsewhere. For example, silicon isotopes are excellent markers of evaporation processes and climatic changes. Additionally, the types of vegetation that grow on ultramafic soils as a function of climate are highly adapted and include both Ni hyperaccumulative species, which can accumulate several per cent by weight of Ni, and non-accumulative species. Estrade et al. [67] have shown that the isotopic compositions of plants growing on these soils tend to be isotopically heavier than that of the soil itself, suggesting that the fraction of dissolved Ni controlled by weathering carries a heavy isotopic signature. Future studies should explore whether very superficial processes influence deeper processes in the laterite profile and whether they result in a particular isotopic signature.

The geometry and permeability of the network primarily govern the weathering front. However, the alteration process also induces changes in porosity and permeability, which can, in turn, impact redistribution phenomena. Significant progress has been made in understanding boulder development and nickel redistribution. Boulder size can thus be predicted at different scales by assessing fracture networks based on their Peclet and Damkohler numbers. Fracture networks with spacing exceeding the threshold corresponding to a Peclet number of 10 can generate boulders, which are hierarchically organised according to the size of the fracture network responsible for their formation.

The study of the impact of fracturing on the progression of the alteration front and nickel redistribution shows that the spatial organisation of alteration and Ni heterogeneities is controlled by fracture spacing and inherited fracture networks. As fracture spacing tends to follow a scaling law, it would be possible to establish a corresponding scaling law for Ni heterogeneities. Such laws could then be used to develop probabilistic models to predict the characteristic spacing of enriched zones. Additionally, scaling laws for mineralisation could be formulated to inform probabilistic models predicting the distribution (frequency) of altered zones at different scales.

To accurately replicate the evolution of porosity, permeability, and compaction, it will be essential to incorporate mechanical coupling, which presents significant numerical challenges. Furthermore, the periodic desaturation of networks, which affects silicate saturation, must be accounted for in the models.

Transitioning to 3D models, which will require parallel processing, will enable the exploration of more complex flows and the development of a more realistic geometric and hydrodynamic model. This model will allow a more rigorous testing of conceptual models, considering fracture networks and a more complex topographic evolution. This will require mining operators to provide a detailed structural description of the deposits with systematic measurement of faults and join networks; data that are often lacking.

Author Contributions: Conceptualisation, M.C., Y.T., J.-L.G. and F.G.; methodology, M.C., J.-L.G., E.R., S.F., M.M. and M.U.; software, J.-L.G. and S.F.; analysis: M.C., Y.T., S.F., J.-L.G., Y.K., S.G., M.M., M.U., J.J. and S.É.; writing—original draft preparation, M.C., Y.T., J.-L.G. and M.M.; review and editing, all authors; supervision, M.C., Y.T., J.-L.G. and F.G.; project administration, M.C. and Y.T.; funding acquisition, M.C. and Y.T. All authors have read and agreed to the published version of the manuscript.

Funding: This work has been funded and logistically supported by the CNRT research contract CSF N° 9PS2017-CNRT.GEORESSOURCE/TRANSNUM «Facteurs d'enrichissements et transferts de Ni, Co-Sc dans les saprolites de Nouvelle Calédonie: approche géométrique, minéralo-géochimique et numérique», and by the French National Research Agency (ANR) through the national program "Investissements d'avenir" of the Labex Ressources 21 with the reference ANR-10-LABX-21-01/LABEX RESSOURCES21.

Data Availability Statement: Data are available in the CNRT final report of the contract mentioned above ("Transnum"), which is open access on the CNRT's website.

Acknowledgments: The authors would like to thank Andreï Lecomte for SEM images, J. Gambaja for TEM imaging (SCMEM, GeoRessources, Vandœuvre-lès-Nancy, France), Fabienne Warmont (CNRS-Orléans) as well as MC Boiron, and C. Peiffert (LA-ICP-MS facilities, GeoRessources), for technical support. Sampling benefited from the help of several mine geologists during sampling (Koniambo, SMT, SLN).

Conflicts of Interest: The authors declare no conflicts of interest.

References

1. Nahon, D.; Tardy, Y. The Ferruginous Laterites. In *Handbook of Exploration Geochemistry*; Elsevier: Amsterdam, The Netherlands, 1992; pp. 41–55. [CrossRef]
2. Golightly, J.-P. Progress in Understanding the Evolution of Nickel Laterites. in The Challenge of Finding New Mineral Resources Global Metallogeny, Innovative Exploration, and New Discoveries. *Soc. Econ. Geol. Spec. Publ.* **2010**, *15*, 451–475.

3. Thorne, R.; Herrington, R.; Robert, S. Composition and origin of the Çaldag oxide nickel laterite, W. Turkey. *Miner. Depos.* **2009**, *44*, 581–595. [CrossRef]
4. Vasconcelos, P.M.; Reich, M.; Shuster, D.L. The Paleoclimatic Signatures of Supergene Metal Deposits. *Elements* **2015**, *11*, 317–322. [CrossRef]
5. Anand, R.R. Regolith-landform processes and geochemical exploration for base metal deposits in regolith-dominated terrains of the Mt Isa region, northwest Queensland, Australia. *Ore Geol. Rev.* **2016**, *73*, 451–474. [CrossRef]
6. Reis, F.D.A.A.; Brantley, S.L. Models of transport and reaction describing weathering of fractured rock with mobile and immobile water. *J. Geophys. Res. Earth Surf.* **2017**, *122*, 735–757. [CrossRef]
7. Tardy, Y.; Roquin, C. Geochemistry and evolution of lateritic landscapes. In *Developments in Earth Surface Processes*; Elsevier: Amsterdam, The Netherlands, 1992; Volume 2, pp. 407–443.
8. Butt, C.R.M.; Cluzel, D. Nickel Laterite Ore Deposits: Weathered Serpentinites. *Elements* **2013**, *9*, 123–128. [CrossRef]
9. Grimaud, J.L. Dynamique Long-Terme de L'érosion en Contexte Cratonique: L'Afrique de l'Ouest depuis l'Eocène. Ph.D. Thesis, Université Paul Sabatier-Toulouse II, Toulouse, France, 2014.
10. Beauvais, A.; Chardon, D. Modes, tempo, and spatial variability of Cenozoic cratonic denudation: The West African example. *Geochem. Geophys.* **2013**, *14*, 1590–1608. [CrossRef]
11. Jean, A.; Beauvais, A.; Chardon, D.; Arnaud, N.; Jayananda, M.; Mathe, P.E. Weathering history and landscape evolution of Western Ghats (India) from 40Ar/39Ar dating of supergene K–Mn oxides. *J. Geol. Soc.* **2020**, *177*, 523–536. [CrossRef]
12. Elias, M. Nickel laterite deposits-geological overview, resources and exploitation. In *Giant Ore Deposits: Characteristics, Genesis and Exploration*; Cooke, D.R., Pongratz, J., Eds.; Special Publication; Centre for Ore Deposit Research, University of Tasmania: Hobart, Australia, 2002; Volume 4, pp. 205–220.
13. Favier, S.; Teitler, Y.; Golfier, F.; Cathelineau, M. Multiscale physical-chemical analysis of the impact of fracture networks on weathering: Application to nickel redistribution in the formation of Ni-laterite ores, New Caledonia. *Ore Geol. Rev.* **2022**, *147*, 104971. [CrossRef]
14. Cathelineau, M.; Boiron, M.C.; Grimaud, J.L.; Favier, S.; Teitler, Y.; Golfier, F. Pseudo-Karst Silicification Related to Late Ni Reworking in New Caledonia. *Minerals* **2023**, *13*, 518. [CrossRef]
15. Sevin, B.; Cluzel, D.; Maurizot, P.; Ricordel-Prognon, C.; Chaproniere, G.; Folcher, N.; Quesnel, F. A drastic lower Miocene regolith evolution triggered by post-obduction slab break-off and uplift in New Caledonia. *Tectonics* **2014**, *33*, 1787–1801. [CrossRef]
16. Teitler, Y.; Cathelineau, M.; Ulrich, M.; Ambrosi, J.P.; Munoz, M.; Sevin, B. Petrology and geochemistry of scandium in New Caledonian Ni-Co laterites. *J. Geochem. Explor.* **2019**, *196*, 131–155. [CrossRef]
17. Teitler, Y.; Favier, S.; Ambrosi, J.-P.; Sevin, B.; Golfier, F.; Cathelineau, M. Evaluation of Sc Concentrations in Ni-Co Laterites Using Al as a Geochemical Proxy. *Minerals* **2022**, *12*, 615. [CrossRef]
18. Cathelineau, M.; Quesnel, B.; Gautier, P.; Boulvais, P.; Couteau, C.; Drouillet, M. Nickel dispersion and enrichment at the bottom of the regolith: Formation of pimelite target-like ores in rock block joints (Koniambo Ni deposit, New Caledonia). *Miner. Depos.* **2016**, *51*, 271–282. [CrossRef]
19. Cathelineau, M.; Myagkiy, A.; Quesnel, B.; Boiron, M.-C.; Gautier, P.; Boulvais, P.; Ulrich, M.; Truche, L.; Golfier, F.; Drouillet, M. Multistage crack seal vein and hydrothermal Ni enrichment in serpentinised ultramafic rocks (Koniambo massif, New Caledonia). *Miner. Depos.* **2017**, *52*, 945–960. [CrossRef]
20. Villanova-de-Benavent, C.; Jawhari, T.; Roqué-Rosell, J.; Galí, S.; Proenza, J.A. Ni-bearing phyllosilicates ("garnierites"): New insights from thermal analysis, μRaman and IR spectroscopy. *Appl. Clay Sci.* **2019**, *175*, 47–66. [CrossRef]
21. Dublet, G.; Juillot, F.; Morin, G.; Fritsch, E.; Fandeur, D.; Ona-Nguema, G.; Brown, G.E. Ni speciation in a New Caledonian lateritic regolith: A quantitative X-Ray absorption spectroscopy investigation. *Geochim. Cosmochim. Acta* **2012**, *95*, 119–133. [CrossRef]
22. Muñoz, M.; Ulrich, M.; Cathelineau, M.; Mathon, O. Weathering processes and crystal chemistry of Ni-bearing minerals in saprock horizons of New Caledonia ophiolite. *J. Geochem. Explor.* **2019**, *198*, 82–99. [CrossRef]
23. Dublet, G.; Juillot, F.; Morin, G.; Fritsch, E.; Fandeur, D.; Brown, G.E. Goethite ageing explains Ni depletion in upper units of ultramafic lateritic ores from New Caledonia. *Geochim. Cosmochim. Acta* **2015**, *160*, 1–15. [CrossRef]
24. Ramanaidou, E.R.; Wells, M.A.; Godel, B. Ni-goethites in nickel laterites. In Proceedings of the International Workshop Geochemical Cycle of Ni, Co and Sc: From Mining Exploration to Ecotoxicity, Nancy, France, 17–19 October 2017.
25. Quesnel, B.; de Veslud, C.L.C.; Boulvais, P.; Gautier, P.; Cathelineau, M.; Drouillet, M. 3D modeling of the laterites on top of the Koniambo Massif, New Caledonia: Refinement of the per descensum lateritic model for nickel mineralisation. *Miner. Depos.* **2017**, *52*, 961–978. [CrossRef]
26. Fritsch, E.; Juillot, F.; Dublet, G.; Fonteneau, L.; Fandeur, D.; Martin, E.; Caner, L.; Auzende, A.-L.; Grauby, O.; Beaufort, D. An Alternative Model for the Formation of Hydrous Mg/Ni Layer Silicates ('deweylite'/'garnierite') in Faulted Peridotites of New Caledonia: I. Texture and Mineralogy of a Paragenetic Succession of Silicate Infillings. *Eur. J. Mineral.* **2016**, *28*, 295–311. [CrossRef]
27. Wells, M.A.; Ramanaidou, E.R.; Verrall, M.; Tessarolo, C. Mineralogy and chemical chemistry of 'garnierites' in the Goro lateritic nickel deposit, New Caledonia. *Eur. J. Mineral.* **2009**, *21*, 467–483. [CrossRef]

28. Trescases, J.J. L'évolution Géochimique Supergène des Roches Ultrabasiques en Zone Tropicale: Formation des Gisements Nickélifères de Nouvelle-Calédonie, 1975, Mémoires ORSTOM (Office de La Recherche Scientifique et Technique Outre-Mer) n°78, 278p, no AO8708: 1973/09/26, ISBN 2-7099-0362-8. Available online: https://horizon.documentation.ird.fr/exl-doc/pleins_textes/pleins_textes_6/Mem_cm/07526.pdf (accessed on 26 August 2024).
29. Chardon, D.; Chevillotte, V. Morphotectonic evolution of the New Caledonia ridge (Pacific Southwest) from post-obduction tectonosedimentary record. *Tectonophysics* **2006**, *420*, 473–491. [CrossRef]
30. Chevillotte, V. Morphogenèse Tropicale en contexte Epirogénique Modéré: Exemple de la Nouvelle-Calédonie (Pacifique Sud-Ouest). Ph.D. Thesis, Université de la Nouvelle-Calédonie, Nouméa, New Caledonia, France, 2005.
31. Maurizot, P.; Lafoy, Y.; Poupée, M. Cartographie des Formations Superficielles et des aléas Mouvements de Terrain en Nouvelle-Calédonie, Zone du Koniambo. BRGM, Public Report RP51624-FR, 2002; 45p. Available online: http://infoterre.brgm.fr/rapports/RP-51624-FR.pdf (accessed on 26 August 2024).
32. Maurizot, P.; Sevin, B.; Lesimple, S.; Bailly, L.; Iseppi, M.; Robineau, B. Mineral resources and prospectivity of the ultramafic rocks of New Caledonia, Chapter 10. *Geol. Soc. Lond. Mem.* **2020**, *51*, 247–277. [CrossRef]
33. Sevin, B. Cartographie du Régolithe sur Formation Ultrabasique de Nouvelle-Calédonie: Localisation dans l'espace et le Temps des Gisements Nickélifères. Ph.D. Thesis, Université de la Nouvelle-Calédonie, Nouméa, New Caledonia, 2014.
34. Sevin, B.; Maurizot, P.; Cluzel, D.; Tournadour, E.; Etienne, S.; Folcher, N.; Patriat, M. Post-obduction evolution of New Caledonia. *Geol. Soc. Lond. Mem.* **2020**, *51*, 147–188, Chapter 7. [CrossRef]
35. Iseppi, M.; Sevin, B.; Cluzel, D.; Maurizot, P.; Bayon, B.L. Supergene nickel ore deposits controlled by gravity-driven faulting and slope failure, Peridotite Nappe, New Caledonia. *Econ. Geol.* **2018**, *113*, 531–544. [CrossRef]
36. Sevin, B.; Ricordel-Prognon, C.; Quesnel, B.; Cluzel, D.; Lesimple, S.; Maurizot, P. First palaeomagnetic dating of ferricrete in New Caledonia: New insight on the morphogenesis and palaeoweathering of 'Grande Terre'. *Terra Nova* **2012**, *24*, 77–85. [CrossRef]
37. Jeanpert, J. Structural and Hydrogeologic Characterisation of the Peridotitic Massifs of New Caledonia. Ph.D. Thesis, Université de la Réunion, Saint-Denis, Réunion, 2017.
38. Jeanpert, J.; Iseppi, M.; Adler, P.M.; Genthon, P.; Sevin, B.; Thovert, J.-F.; Dewandel, B.; Join, J.-L. Fracture controlled permeability of ultramafic basement aquifers. Inferences from the Koniambo massif, New Caledonia. *Eng. Geol.* **2019**, *256*, 67–83. [CrossRef]
39. Domènech, C.; Galí, S.; Villanova-de-Benavent, C.; Soler, J.M.; Proenza, J.A. Reactive transport model of the formation of oxide-type Ni-laterite profiles (Punta Gorda, Moa Bay, Cuba). *Miner. Depos.* **2017**, *52*, 993–1010. [CrossRef]
40. Myagkiy, A.; Truche, L.; Cathelineau, M.; Golfier, F. Revealing the conditions of Ni mineralisation in the laterite profiles of New Caledonia: Insights from reactive geochemical transport modelling. *Chem. Geol.* **2017**, *466*, 274–284. [CrossRef]
41. Favier, S.; Teitler, Y.; Golfier, F.; Cathelineau, M. Reactive transport modelling in porous fractured media: Application to weathering processes. *Water Resour. Res.* **2024**, *60*, e2023WR035283. [CrossRef]
42. Cluzel, D.; Maurizot, P.; Collot, J.; Sevin, B. An outline of the geology of New Caledonia; from Permian-Mesozoic Southeast Gondwanaland active margin to Cenozoic obduction and supergene evolution. *Epis.-News Mag. Int. Union Geol. Sci.* **2012**, *35*, 72–86. [CrossRef]
43. Gautier, P.; Quesnel, B.; Boulvais, P.; Cathelineau, M. The emplacement of the Peridotite Nappe of New Caledonia and its bearing on the tectonics of obduction. *Tectonics* **2016**, *35*, 3070–3094. [CrossRef]
44. Pirard, C.; Hermann, J.; O'Neill, H.S.C. Petrology and Geochemistry of the Crust-Mantle Boundary in a Nascent Arc, Massif du Sud Ophiolite, New Caledonia, SW Pacific. *J. Petrol.* **2013**, *54*, 1759–1792. [CrossRef]
45. Ulrich, M.; Picard, C.; Guillot, S.; Chauvel, C.; Cluzel, D.; Meffre, S. Multiple melting stages and refertilization as indicators for ridge to subduction formation: The New Caledonia ophiolite. *Lithos* **2010**, *115*, 223–236. [CrossRef]
46. Quesnel, B.; Gautier, P.; Cathelineau, M.; Boulvais, P.; Couteau, C.; Drouillet, M. The internal deformation of the Peridotite Nappe of New Caledonia: A structural study of serpentine-bearing faults and shear zones in the Koniambo Massif. *J. Struct. Geol.* **2016**, *85*, 51–67. [CrossRef]
47. Ulrich, M.; Muñoz, M.; Boulvais, P.; Cathelineau, M.; Guillot, S.; Picard, C. Serpentinisation of New Caledonia peridotites: From depth to (sub-)surface. *Contrib. Miner. Pet.* **2020**, *175*, 91. [CrossRef]
48. Jeanpert, J.; Dewandel, B. *Analyse Préliminaire des Données Hydrogéologiques du Massif du Koniambo, Nouvelle-Calédonie*; SGNC/DIMENC; Report BRGM/RP-61765-FR; SGNC: Nouméa, New Caledonia, France, 2013; 95p.
49. Chevillotte, V.; Chardon, D.; Beauvais, A.; Maurizot, P.; Colin, F. Long-term tropical morphogenesis of New Caledonia (Southwest Pacific): Importance of positive epeirogeny and climate change. *Geomorphology* **2006**, *81*, 361–375. [CrossRef]
50. Grimaud, J.L.; Chardon, D.; Metelka, V.; Beauvais, A.; Bamba, O. Neogene cratonic erosion fluxes and landform evolution processes from regional regolith mapping (Burkina Faso, West Africa). *Geomorphology* **2015**, *241*, 315–330. [CrossRef]
51. Grimaud, J.L.; Rouby, D.; Chardon, D.; Beauvais, A. Cenozoic sediment budget of West Africa and the Niger Delta. *Basin Res.* **2018**, *30*, 169–186. [CrossRef]
52. Parkhurst, D.L.; Appelo, C. Description of input and examples for PHREEQC version 3—A computer program for speciation, batch-reaction, one-dimensional transport, and inverse geochemical calculations. *US Geol. Surv. Tech. Methods* **2013**, *6*, 497.
53. COMSOL Multiphysics® (5.6). [Computer Software] 2020. COMSOL AB, Stockholm, Sweden. Available online: www.comsol.com (accessed on 15 January 2021).
54. Favier, S.; Teitler, Y.; Golfier, F.; Cathelineau, M. Migration of dissolution front in a fracture network—Implications for weathering of fractured bedrock systems and boulder formation. *J. Hydrol.* **2024**, *644*, 132056. [CrossRef]

55. Maurizot, P.; Vendé-Leclerc, M. *Carte Géologique de la Nouvelle-Calédonie au 1/500 000, 2009*; Direction de l'Industrie, des Mines et de l'Energie, Service de la Géologie de Nouvelle-Calédonie (SGNC); Bureau de Recherches Géologiques et Minières: Nouméa, New Caldonia, France, 2009.
56. Cluzel, D.; Vigier, B. Syntectonic Mobility of Supergene Nickel Ores of New Caledonia (Southwest Pacific). Evidence from Garnierite Veins and Faulted Regolith. *Resour. Geol.* **2008**, *58*, 161–170. [CrossRef]
57. Lagabrielle, Y.; Chauvet, A. The role of extensional faulting in shaping Cenozoic New-Caledonia. *Bull. Soc. Géol. Fr.* **2008**, *179*, 315–329. [CrossRef]
58. Genna, A.; Maurizot, P.; Lafoy, Y.; Augé, T. Contrôle karstique de minéralisations nickélifères de Nouvelle-Calédonie. *C. R. Geosci.* **2005**, *337*, 367–374. [CrossRef]
59. Farrokhpay, F.; Cathelineau, M.; Blancher, S.; Laugier, O.; Filippov, L. Characterization of Weda Bay nickel laterite ore from Indonesia. *J. Geochem. Explor.* **2019**, *196*, 270–281. [CrossRef]
60. Muñoz, M.; Ulrich, M.; Cathelineau, M.; Mathon, O. Crystal Chemistry and Concentration Process of Nickel in New Caledonia laterite. Goldschmidt Conference Hawai, 2022, Session 8h, Raw Materials for a Low Carbon Future 302A/B. Available online: https://conf.goldschmidt.info/goldschmidt/2022/meetingapp.cgi/Paper/10128 (accessed on 26 August 2024).
61. Idnurm, M.; Senior, B.R. Palaeomagnetic ages of late Cretaceous and Tertiary weathered profiles in the Eromanga Basin, Queensland. *Palaeogeogr. Palaeoclimatol. Palaeoecol.* **1978**, *24*, 263–272. [CrossRef]
62. Radtke, U.; Brückner, H. Investigation on age and genesis of silcretes in Queensland (Australia)-Preliminary results. *Earth Surf. Process. Landf.* **1991**, *16*, 547–554. [CrossRef]
63. Mathian, M.; Chassé, M.; Calas, G.; Griffin, W.L.; O'Reilly, S.Y.; Buisson, T.; Allard, T. Insights on the Cenozoic climatic history of Southeast Australia from kaolinite dating. *Palaeogeogr. Palaeoclimatol. Palaeoecol.* **2022**, *604*, 111212. [CrossRef]
64. Lagabrielle, Y.; Maurizot, P.; Lafoy, Y.; Cabioch, G.; Pelletier, B.; Regnier, M.; Wabete, I.; Calmant, S. Post-Eocene extensional tectonics in southern New-Caledonia (SW Pacific): Insights from onshore fault analysis and offshore seismic data. *Tectonophysics* **2005**, *403*, 1–28. [CrossRef]
65. Myagkiy, A.; Golfier, F.; Truche, L.; Cathelineau, M. Reactive Transport Modeling Applied to Ni Laterite Ore Deposits in New Caledonia: Role of Hydrodynamic Factors and Geological Structures in Ni Mineralization. *Geochem. Geophys. Geosyst.* **2019**, *20*, 1425–1440. [CrossRef]
66. Huysmans, M.; Dassargues, A. Review of the use of Péclet numbers to determine the relative importance of advection and diffusion in low permeability environments. *Hydrogeol. J.* **2005**, *13*, 895–904. [CrossRef]
67. Estrade, N.; Cloquet, C.; Echevarria, G.; Sterckeman, T.; Deng, T. Weathering and vegetation controls on nickel isotope fractionation in surface ultramafic environments (Albania), Earth Planet. *Sci. Lett.* **2015**, *423*, 24–35. [CrossRef]